Electronic Supplementary Material (ESI) for Journal of Materials Chemistry C.

Supporting Information

Pyridination of Hole Transporting Material in Perovskite Solar Cells Questions the Long-term Stability

Artiom Magomedov,*[a] Ernestas Kasparavičius,[a] Kasparas Rakstys,[b] Sanghyun Paek,[b] Natalia Gasilova,[b] Kristijonas Genevičius,[c] Gytis Juška,[c] Tadas Malinauskas,[a] Mohammad Khaja Nazeeruddin,*[b] and Vytautas Getautis*[a]

a A. Magomedov, E. Kasparavičius, dr. T. Malinauskas, prof. dr. V. Getautis
Department of Organic Chemistry
Kaunas University of Technology
Radvilenu pl. 19, Kaunas 50254, Lithuania
E-mail: artiom.magomedov@ktu.lt; vytautas.getautis@ktu.lt

b K. Rakstys, dr. S. Paek, dr. N. Gasilova, prof. dr. M.K. Nazeeruddin
Group for Molecular Engineering of Functional Material
Institute of Chemical Sciences and Engineering
École Polytechnique Fédérale de Lausanne
CH-1951 Sion, Switzerland
E-mail: mdkhaja.nazeeruddin@epfl.ch

c dr. K. Genevičius, prof. dr. G. Juška
Department of Solid State Electronics
Vilnius University
Sauletekio 9 III k., 10222 Vilnius, Lithuania

Contents

General methods and materials 3
Computational details 3
Synthesis 3
Synthesis of the 1a 4
Synthesis of the V990 5
^{1}H NMR and ^{13}C NMR spectra of V990 6
Oxidation of the V990 9
Pyridination of the V990^{+}(TFSI^{-}) 10
^{1}H NMR and ^{13}C NMR spectra of V990(tBP^{+})(TFSI^{-}) 11
DFT predicted ^{13}C NMR spectra of V990(tBP^{+}) 13
Oxidation of the V886 14
Pyridination of the V886^{2+}(TFSI^{-})$_2$ 15
^{1}H NMR and ^{13}C NMR spectra of V886(tBP^{+})(TFSI^{-}) 17
^{1}H NMR and ^{13}C NMR spectra of V886(tBP^{+})$_2$(TFSI^{-})$_2$ 22
Ionization Potential Measurements 24
Cyclic voltammetry measurements 25
Conductivity 26
UV/vis spectroscopy 27
Perovskite solar cell fabrication and characterization 28
Perovskite solar cell aging 28
MS analysis of the aged device 30
References 33

General methods and materials

Chemicals were purchased from Sigma-Aldrich and TCI Europe and used as received without further purification. Compounds 1a and 1g were synthesized according to the procedures described earlier. ^{1}H and ^{13}C NMR spectra were taken on Bruker Avance III 400 (400 MHz) or Bruker Avance III 700 (700 MHz) spectrometer at room temperature. All the data are given as chemical shifts in δ (ppm). The course of the reactions products was monitored by TLC on ALUGRAM SIL G/UV254 plates and developed with UV light. Silica gel (grade 9385, 230–400 mesh, 60 Å, Aldrich) was used for column chromatography. Elemental analysis was performed with an Exeter Analytical CE-440 elemental analyser, Model 440 C/H/N/. MS analysis was performed using matrix-assisted laser desorption/ionization time-of-flight (MALDI-TOF) Autoflex instrument from Bruker, while high resolution MS/MS data were obtained with Q Exactive HF Hybrid Quadrupole Orbitrap instrument equipped with nanoelectrospray ionization (nanoESI) Triversa Nanomate source from Advion. All measurements were done in positive polarity.

Computational details

The theoretical calculations were performed using TURBOMOLE version 7.0 software[1]. Molecular structures of the **V990^{+}** and **V990(tBP^{+})** were optimized using Becke's three parameter functional, B3LYP[2,3], and def2-SVP[4,5] basis set in vacuum. Optimized structure and molecular orbitals were visualized with TmoleX version 4.1 software[6].

^{13}NMR spectra of **V990(tBP^{+})** was predicted by means of GIAO DFT method, using B3LYP/def2-SVP level of theory, and tetramethylsilane (TMS) as a reference. For the simplicity, solvent and anion effects were omitted.

Synthesis

Material V886 was synthesized according to an earlier described procedure[7].

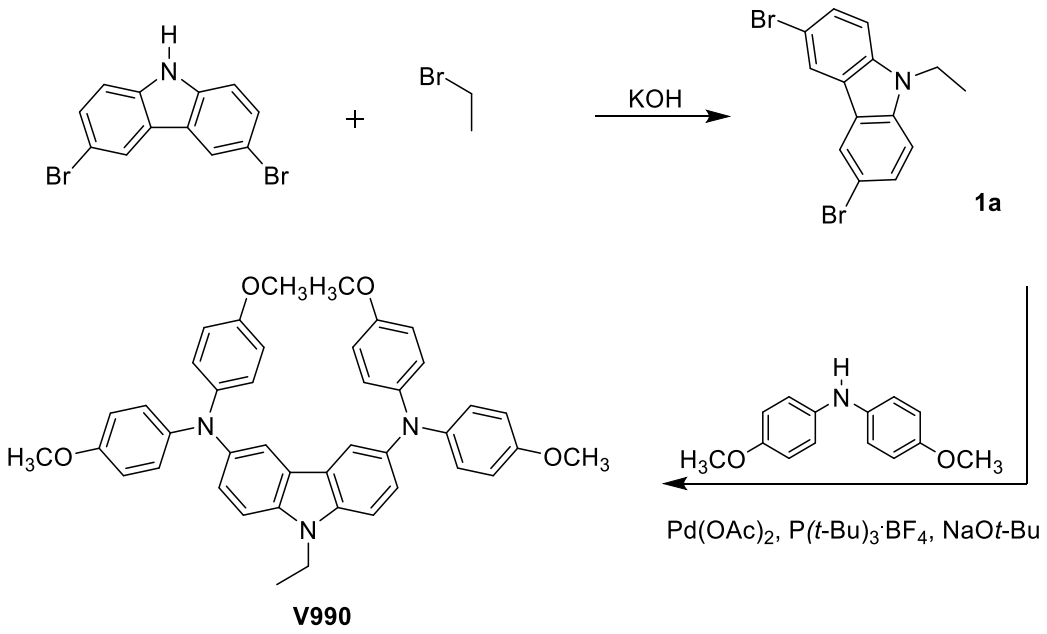

Scheme S1. Synthesis of the **V990**

Synthesis of the 1a

3,6-dibromo-9-ethyl-9H-carbazole; ***1a***

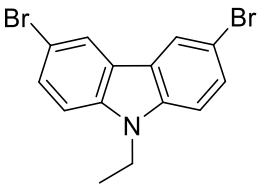

To a solution of 3,6-dibromo-9*H*-carbazole (2 g, 6.15 mmol) and iodoethane (0.64 ml, 8 mmol) in dimethyl sulfoxide (20 ml) powdered KOH was added (1 g). The reaction mixture was stirred at room temperature (25°C) for 2 h, and after reaction completion (TLC, acetone:*n*-hexane 1:4 v:v) distilled water (H_2O_{dist}) was added. The formed precipitate was filtered off, washed with H_2O_{dist} and isopropanole:*n*-hexane (1:1 v:v) mixture to collect final compound as a white crystalline powder. Yield: 2.04 g, 94% (T_m=143.5-145°C).

^{1}H NMR (400 MHz, $CDCl_3$) δ 8.14 (d, *J* = 1.9 Hz, 2H), 7.51 (dd, *J* = 8.5, 1.9 Hz, 2H), 7.19 (d, *J* = 8.5 Hz, 2H), 4.20 (d, *J* = 7.2 Hz, 2H), 1.35 (t, *J* = 7.2 Hz, 3H).

^{13}C NMR (101 MHz, $CDCl_3$) δ 138.73, 128.97, 123.49, 123.25, 111.92, 110.10, 37.79, 13.68.

NMR is in a good agreement with the previously reported data.[8]

Anal. calcd for $C_{14}H_{11}NBr_2$: C, 47.63; H, 3.14; N, 3.97; found: C, 47.52; H, 3.10; N, 3.96.

Synthesis of the V990

3,6-(4,4-dimethoxydiphenylamino)-9-ethyl-9H-carbazole; ***V990***

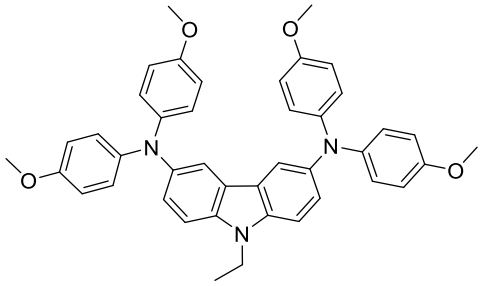

A solution of **1a** (1.76 g, 5 mmol), 4,4'-dimethoxydiphenylamine (3.44 g, 15 mmol) in anhydrous toluene (30 mL) was purged with argon for 20 minutes. Afterwards, palladium(II) acetate (13.4 mg, 0.06 mmol), tri-*tert*-butylphosphonium tetrafluoroborate (23.2 mg, 0.08 mmol) and sodium *tert*-butoxide (1.44 g, 15 mmol) were added and the solution was refluxed under argon atmosphere for 20 hours. After cooling to room temperature, reaction mixture was filtered through Celite. 100 mL of distilled water was added to the filtrate and extraction was done with ethyl acetate. The combined organic layer was dried over anhydrous Na_2SO_4, filtered and solvent evaporated. The crude product was purified by column chromatography using THF:*n*-hexane (1:10 v:v) as eluent. The obtained product was precipitated from 20% solution in THF into 15-fold excess of hexane. The precipitate was filtered off and washed with methanol to collect final compound as a yellow powder. Yield: 1.38 g, 70.3%.

$\underline{R_f}$ =0.16; THF:*n*-hexane (1:10 v:v)

^{1}H NMR (700 MHz, DMSO) δ 7.68 (s, 2H), 7.51 (d, *J* = 8.6 Hz, 2H), 7.12 (d, *J* = 8.1 Hz, 2H), 6.89 – 6.77 (m, 16H), 4.37 (m, 2H), 3.69 (s, 12H), 1.32 (t, *J* = 6.7 Hz, 3H).

^{13}C NMR (176 MHz, DMSO) δ 154.13, 142.11, 139.91, 136.73, 124.43, 123.62, 122.65, 117.03, 114.62, 110.10, 55.16, 37.10, 13.89.

Anal. calcd for $C_{42}H_{39}N_3O_4$: C, 77.63; H, 6.05; N, 6.47; found: C, 77.50; H, 5.98; N, 6.50.

$C_{42}H_{39}N_3O_4$ [$V990^+$] exact mass = 649.2941 Da, observed mass MALDI-TOF-MS) = 649.314 Da

^{1}H NMR and ^{13}C NMR spectra of V990

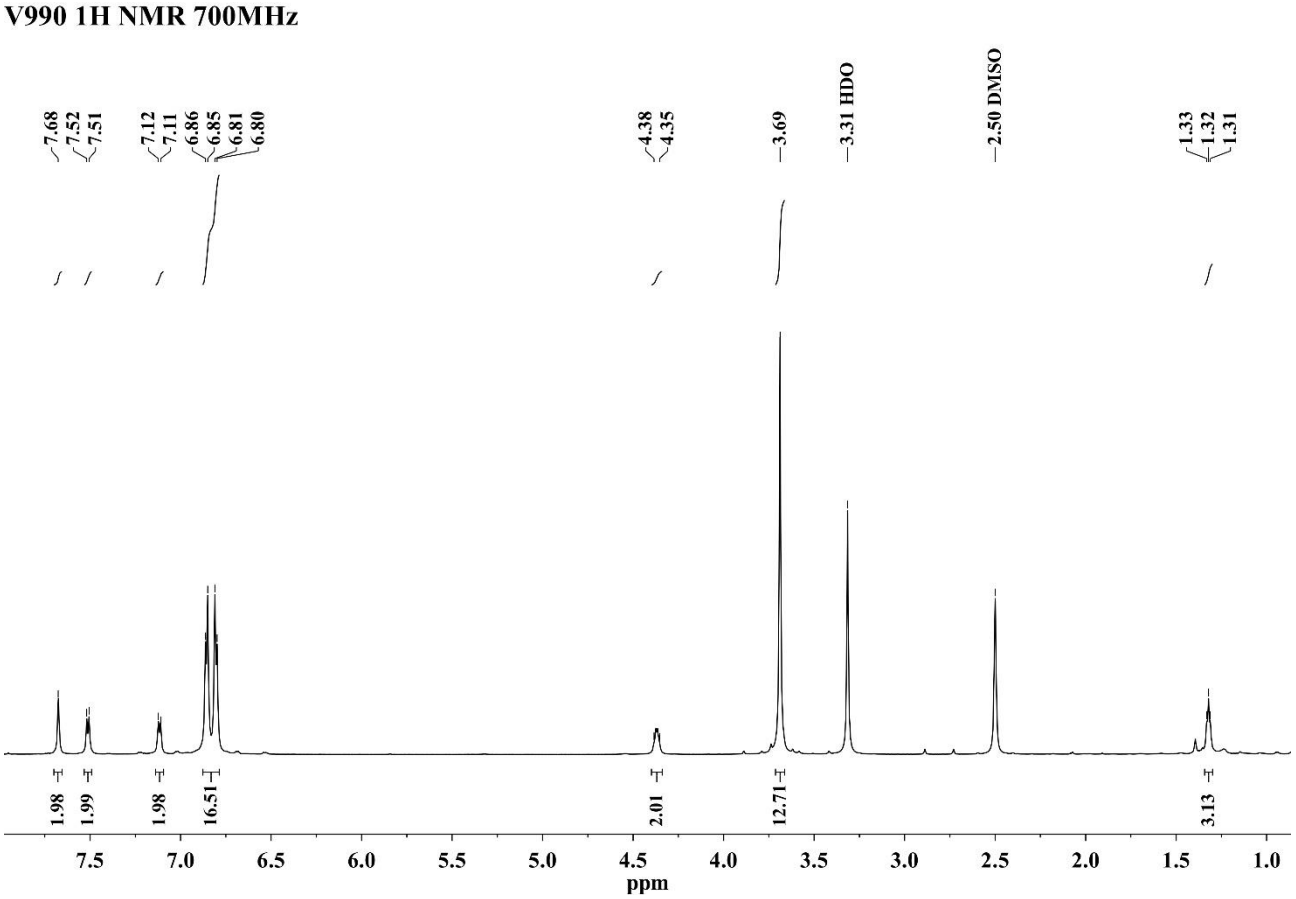

Figure S1. ^{1}H NMR spectrum of **V990** from dmso-d6

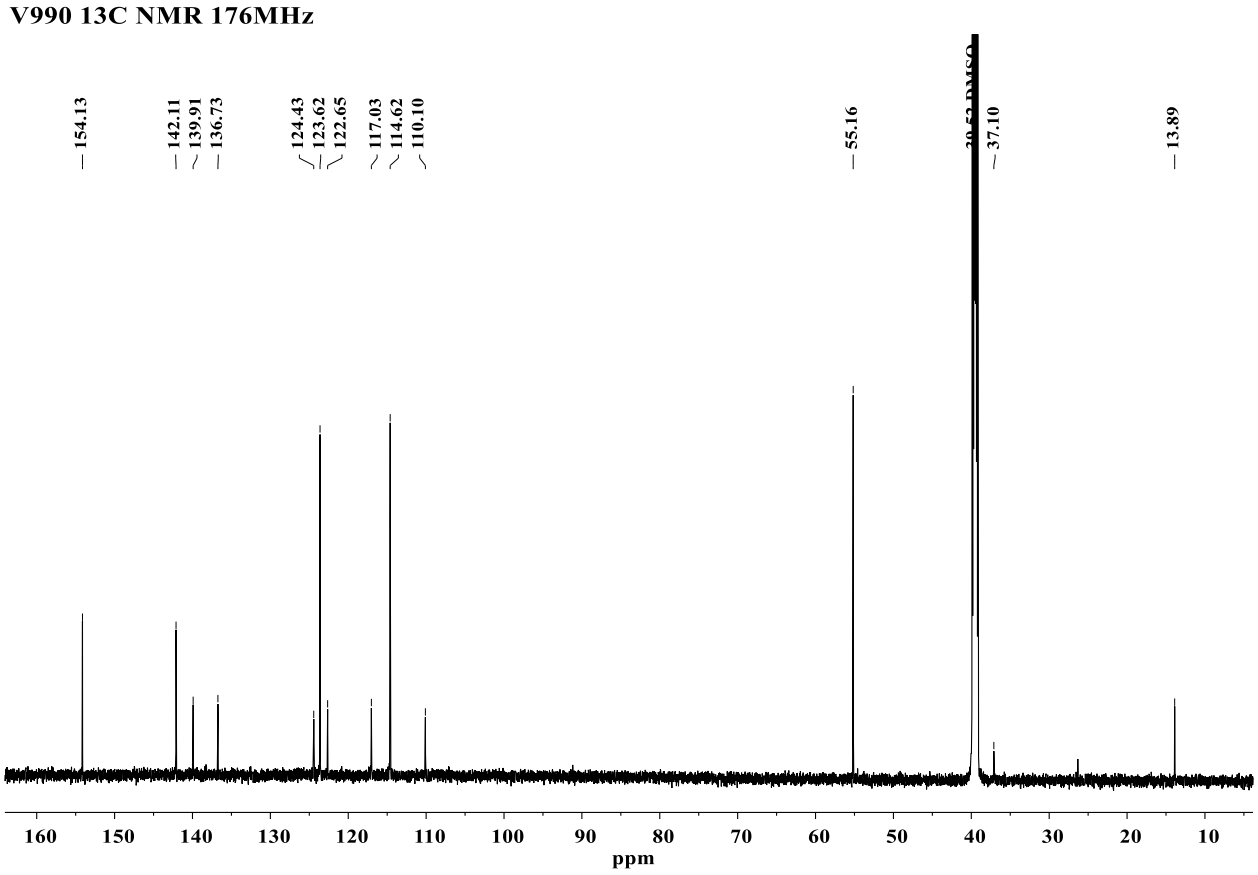

Figure S2. ^{13}C NMR spectrum of **V990** from dmso-d6

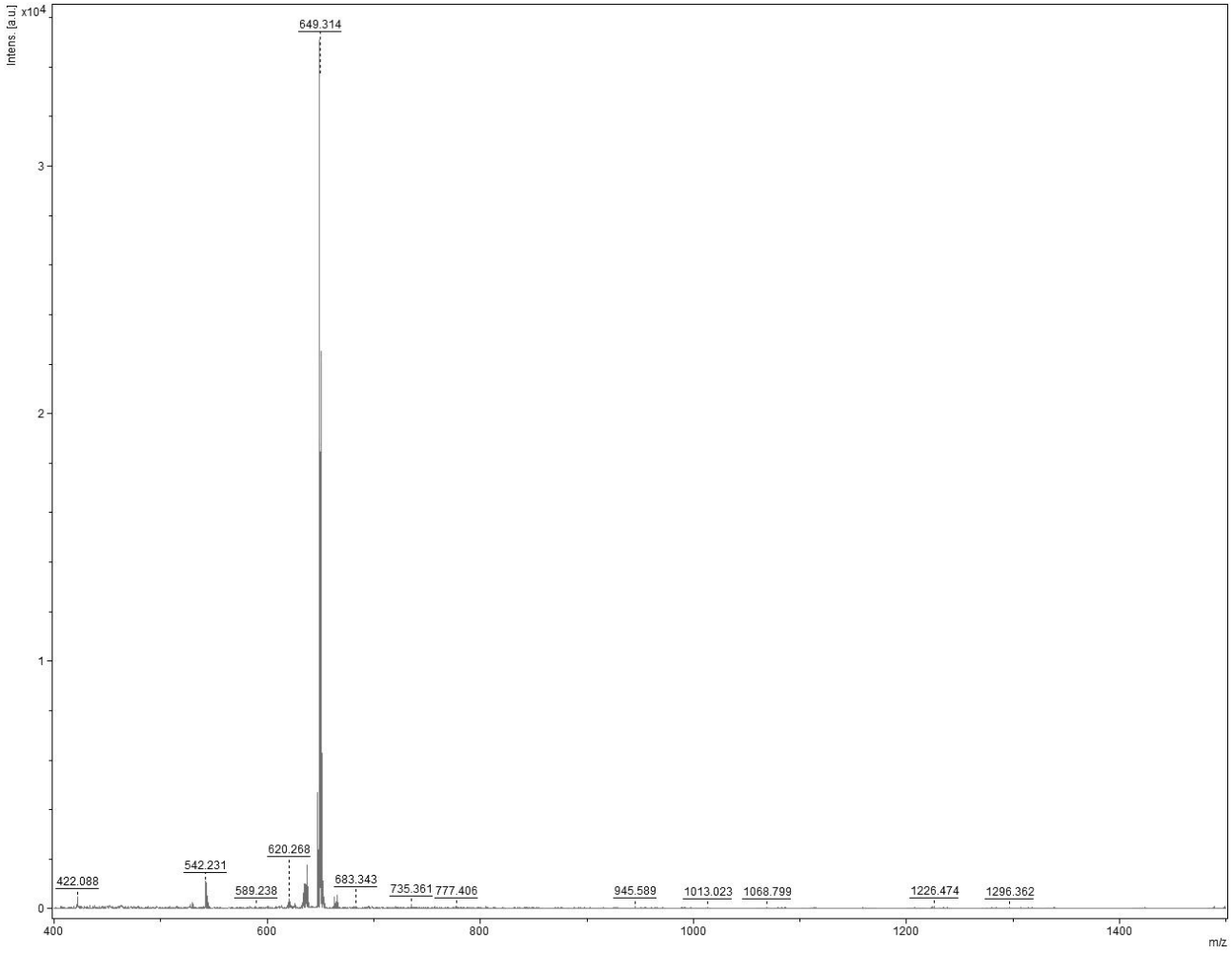

Figure S3. MALDI-TOF-MS spectrum in wide m/z range of **V990**.

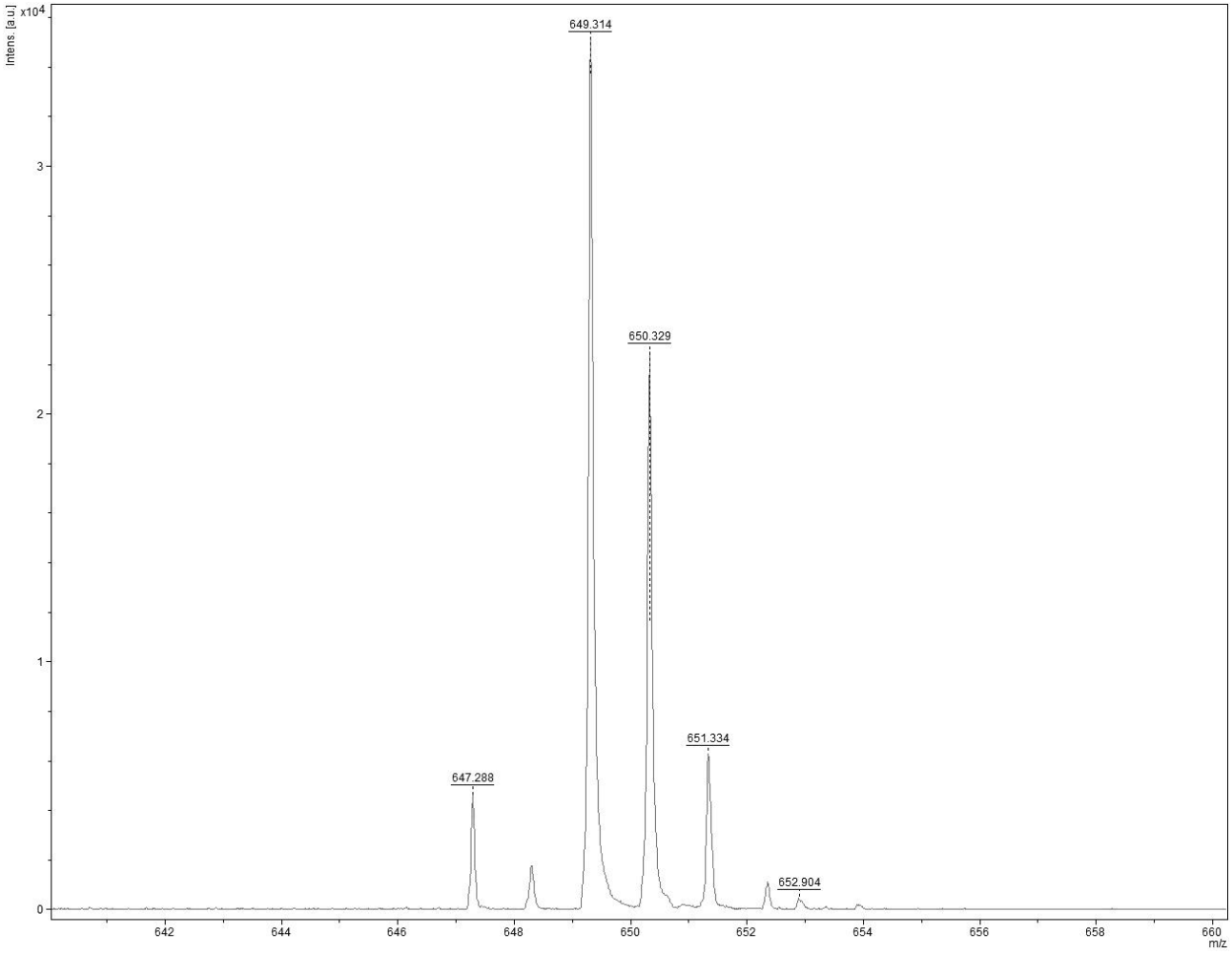

Figure S4. MALDI-TOF-MS spectrum in narrow m/z range of **V990**.

Oxidation of the V990

V990^{+}(TFSI^{-})

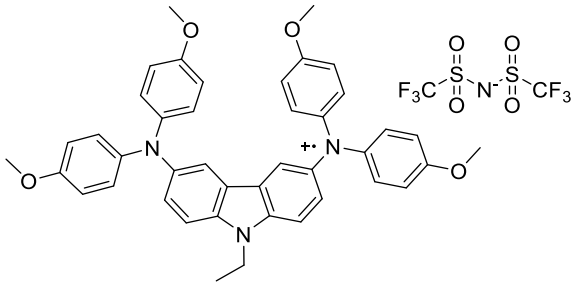

To a 1.38 g (2.12 mmol) of **V990**, dissolved in 75 ml of DCM, 0.82 g (2.12 mmol) of AgTFSI was added. Solution immediately became deep blue-green. After stirring at room temperature for 24 h precipitated silver was filtered off through the plug of celite. DCM was evaporated, and resulting residue was precipitated from 20% solution in DCM into 15-fold excess of ether. The precipitate was filtered off and dried under vacuum resulting in the deep blue-green powder. Yield: 1.62 g, 82.1%.

Anal. calcd for $C_{44}H_{39}F_6N_4O_8S_2$: C, 56.83; H, 4.23; N, 6.02; found: C, 56.67; H, 4.21; N, 6.05.

Pyridination of the V990$^+$(TFSI$^-$)

1-{3,6-bis[bis(4-methoxyphenyl)amino]-9-ethyl-9H-carbazol-4-yl}-4-tert-butylpyridin-1-ium bis(trifluoromethanesulfonyl)azanide; ***V990(tBP$^+$)(TFSI$^-$)***

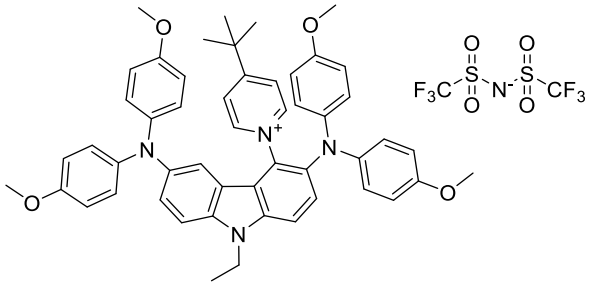

900 mg of **V990$^+$(TFSI$^-$)** was dissolved in 3 ml of the freshly distilled tBP and the resulting solution was heated to 60^{o}C. After 20 min, when color changed from intensive blue-green to dark orange, tBP was distilled off on the rotorvapor. Residue was purified by column chromatography by using acetone:*n*-hexane (1:4 v:v) as eluent, and consequentially strengthening it to the acetone:*n*-hexane (4:1 v:v) eluent. Yield of **V990(tBP$^+$)(TFSI$^-$)**: 397 mg, 38.5%.

Also **V990** was obtained (see full text for the description). Yield of **V990**: 208 mg, 33.0%.

$\underline{R_f}$ =0.06; acetone:*n*-hexane (4:1 v:v)

^{1}H NMR (400 MHz, DMSO) δ 8.98 (d, *J* = 6.5 Hz, 2H), 7.96 (d, *J* = 8.8 Hz, 1H), 7.86 (d, *J* = 6.9 Hz, 2H), 7.64 (d, *J* = 8.9 Hz, 1H), 7.37 (d, *J* = 8.8 Hz, 1H), 7.05 (dd, *J* = 8.8, 2.2 Hz, 1H), 6.81-6.66 (m, 16H), 6.16 (d, *J* = 2.1 Hz, 1H), 4.52 (d, *J* = 7.1 Hz, 2H), 3.73-3.64 (m, 12H), 1.43- 1.34 (m, 3H), 1.19 (s, 9H).

^{13}C NMR (101 MHz, DMSO) δ 172.46, 154.85, 154.60, 146.10, 141.07, 140.80, 140.16, 138.04, 136.03, 133.96, 131.01, 124.95, 124.48, 123.63, 123.46, 121.07, 118.66, 117.88, 116.68, 114.71, 114.66, 55.28, 55.06, 36.33, 29.17, 14.05.

^{13}C NMR (101 MHz, acetone-d6) δ 174.36, 156.61, 156.14, 146.96, 142.83, 142.36, 141.50, 139.46, 137.51, 135.48, 132.05, 127.40, 126.96, 126.40, 125.59, 125.19, 124.68, 122.64, 119.90, 119.44, 118.07, 115.60, 115.44, 114.36, 114.32, 111.75, 55.82, 55.62, 38.65, 37.50, 14.37.

Anal. calcd for $C_{53}H_{51}F_6N_5O_8S_2$: C, 59.82; H, 4.83; N, 6.58; found: C, 59.71; H, 4.86; N, 6.54.

$C_{51}H_{51}N_4O_4^+$ [V990(tBP$^+$)] exact mass = 783.3910 Da, observed mass (MALDI-TOF-MS) = 783.394 Da.

^{1}H NMR and ^{13}C NMR spectra of V990(tBP^{+})(TFSI^{-})

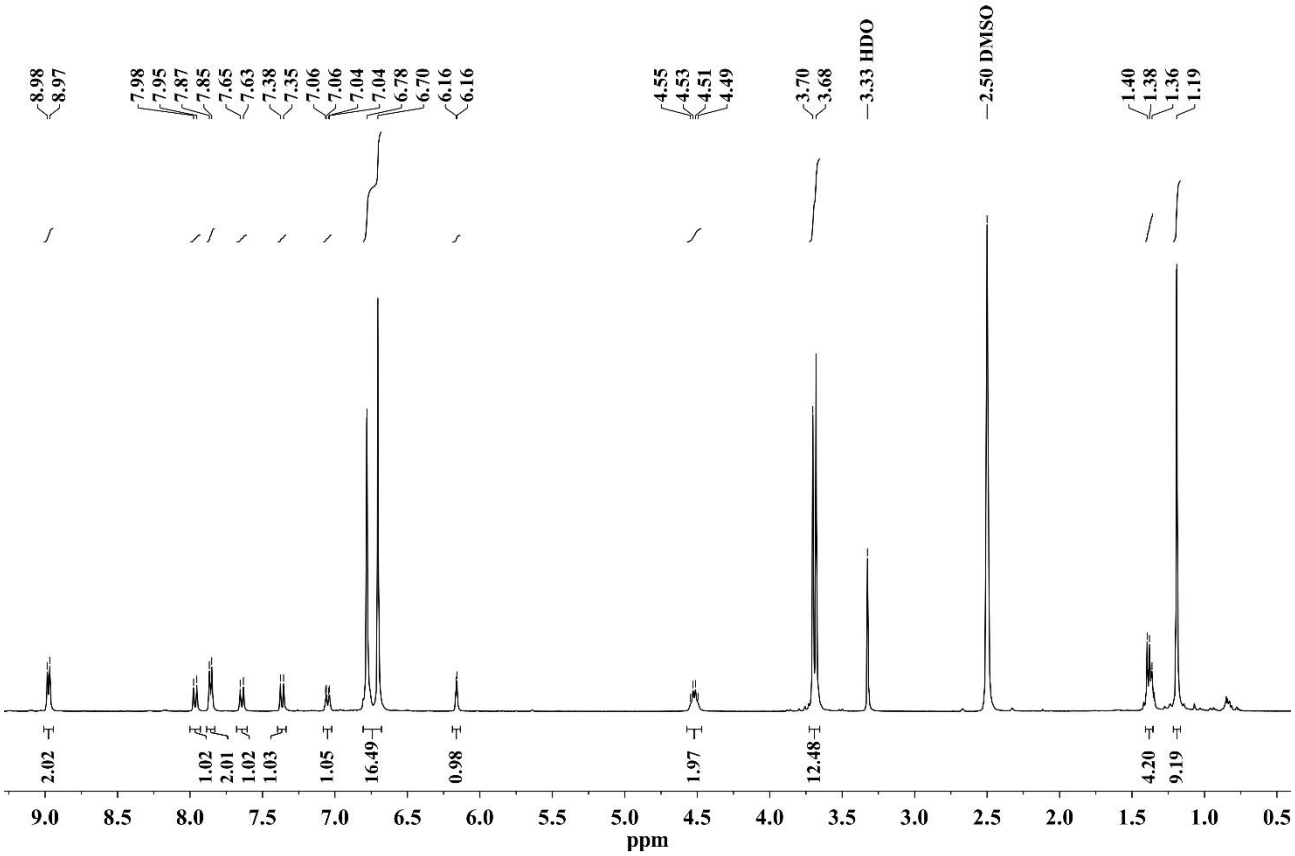

Figure S5. ^{1}H NMR spectrum of **V990(tBP^{+})(TFSI^{-})** from dmso-d6

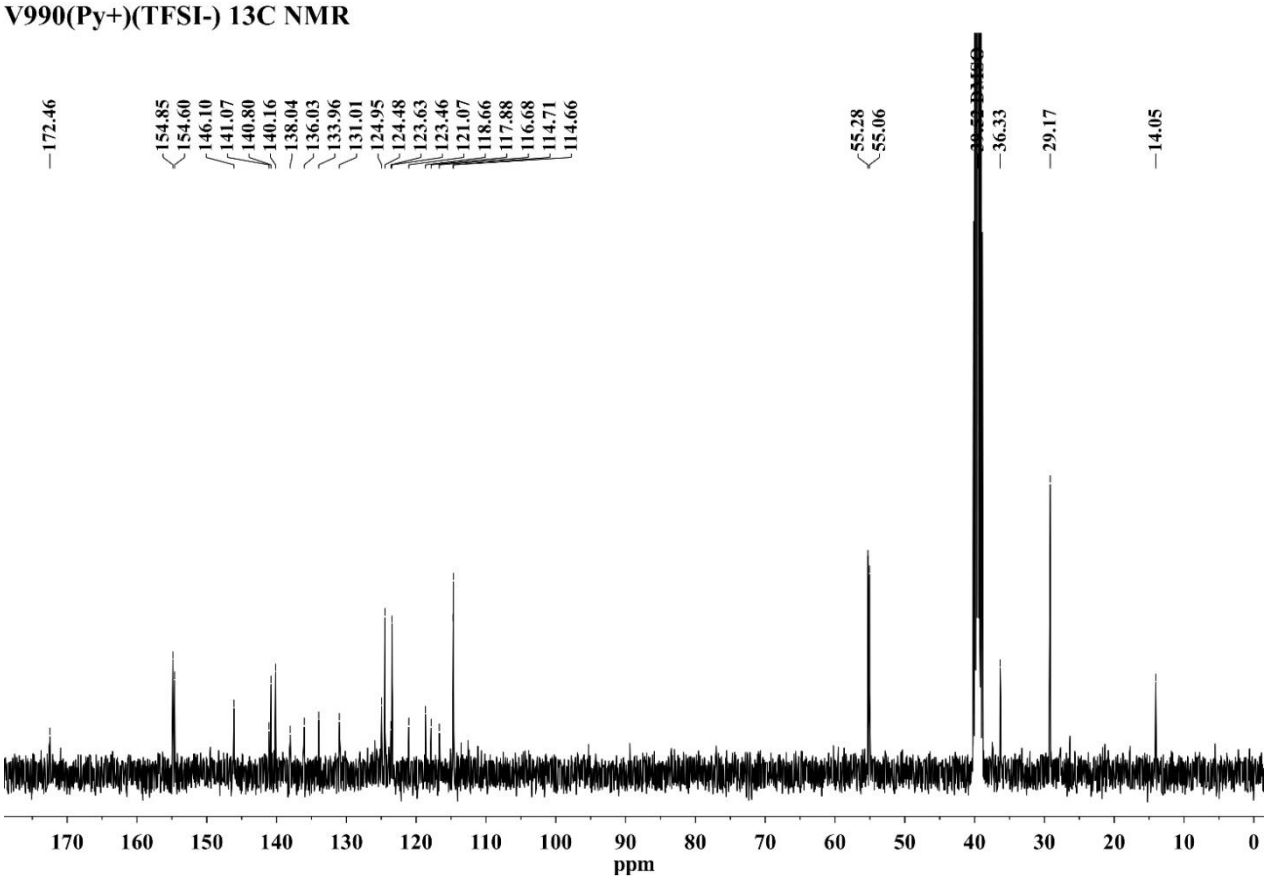

Figure S6. ^{13}C NMR spectrum of **V990(tBP^{+})(TFSI^{-})** from dmso-d6

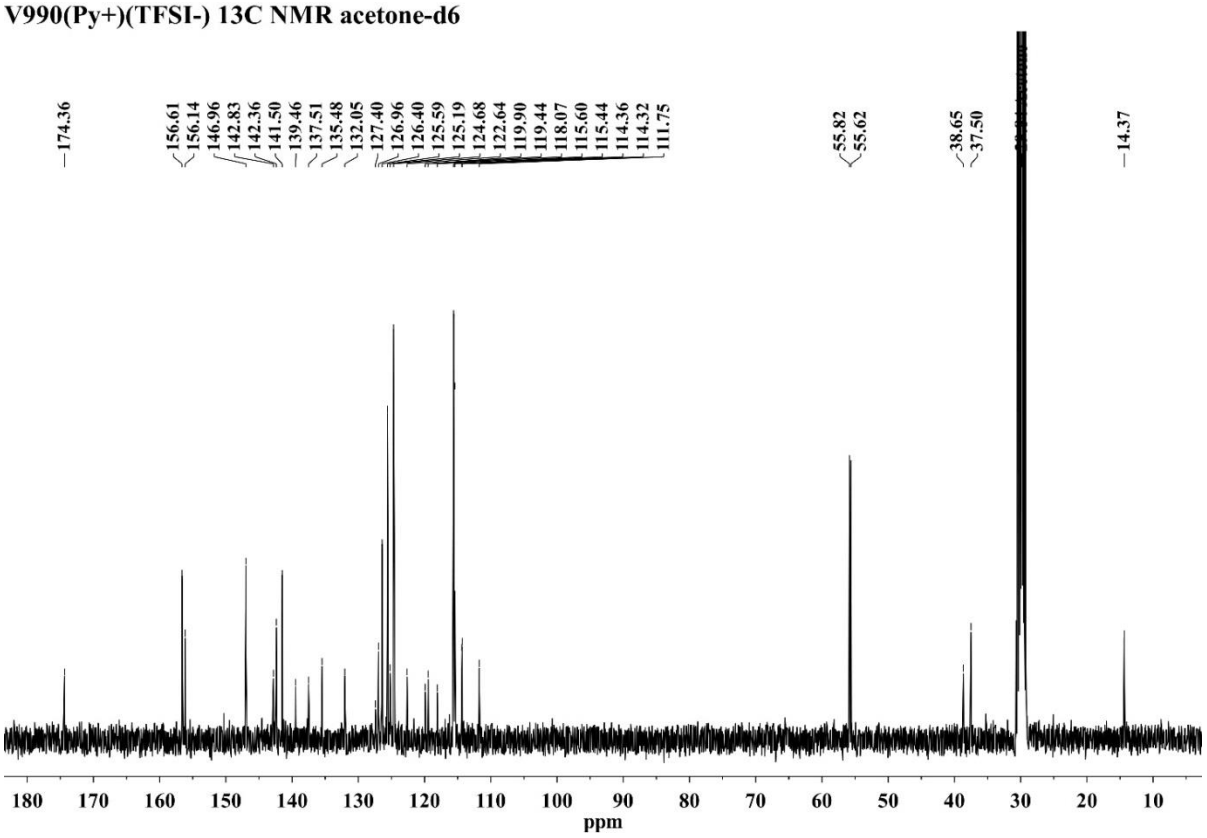

Figure S7. ^{13}C NMR spectrum of **V990(tBP^{+})(TFSI^{-})** from acetone-d6

DFT predicted ^{13}C NMR spectra of V990(tBP^{+})

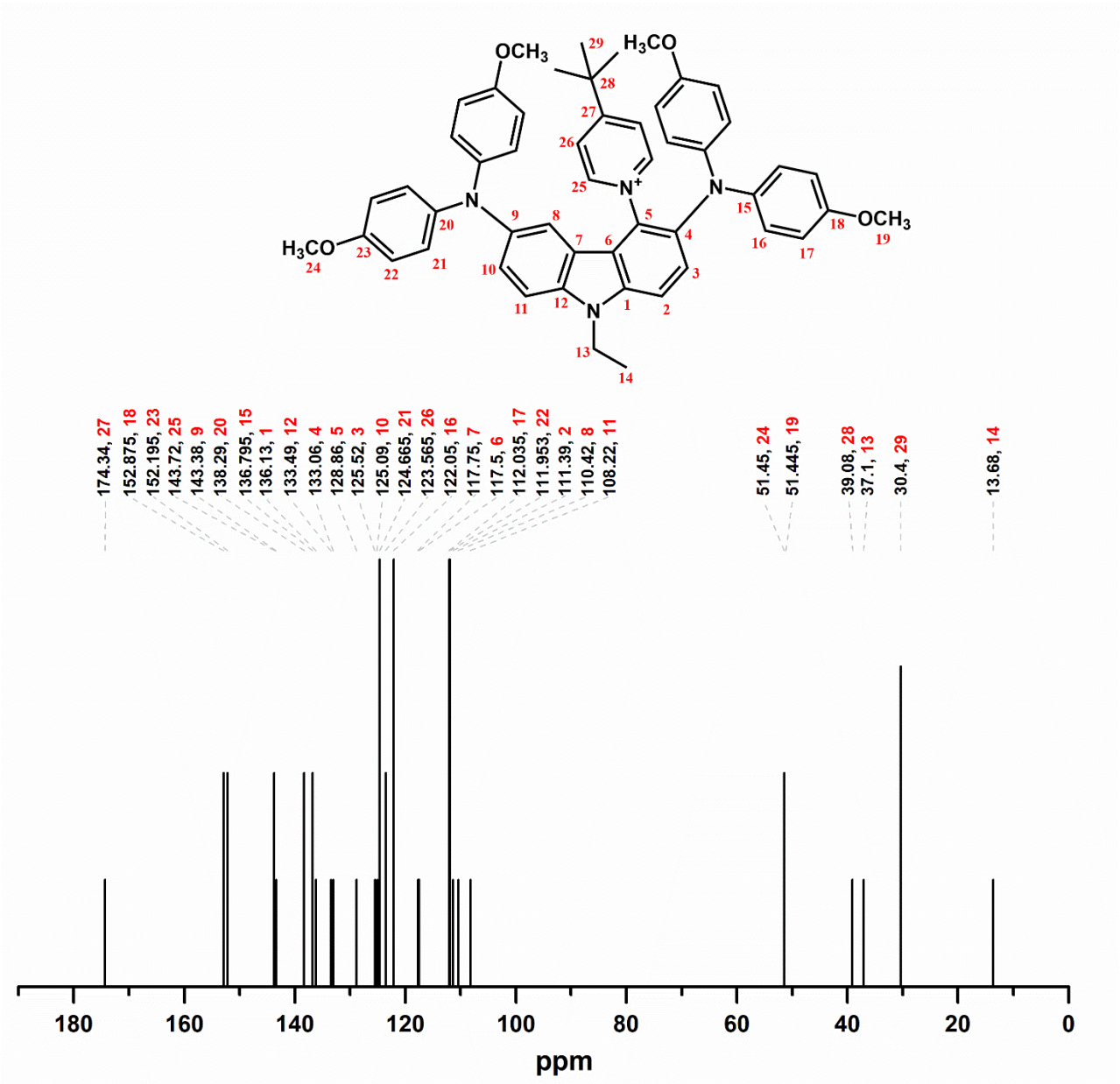

Figure S8. DFT predicted ^{13}C NMR spectrum of **V990(tBP^{+})**

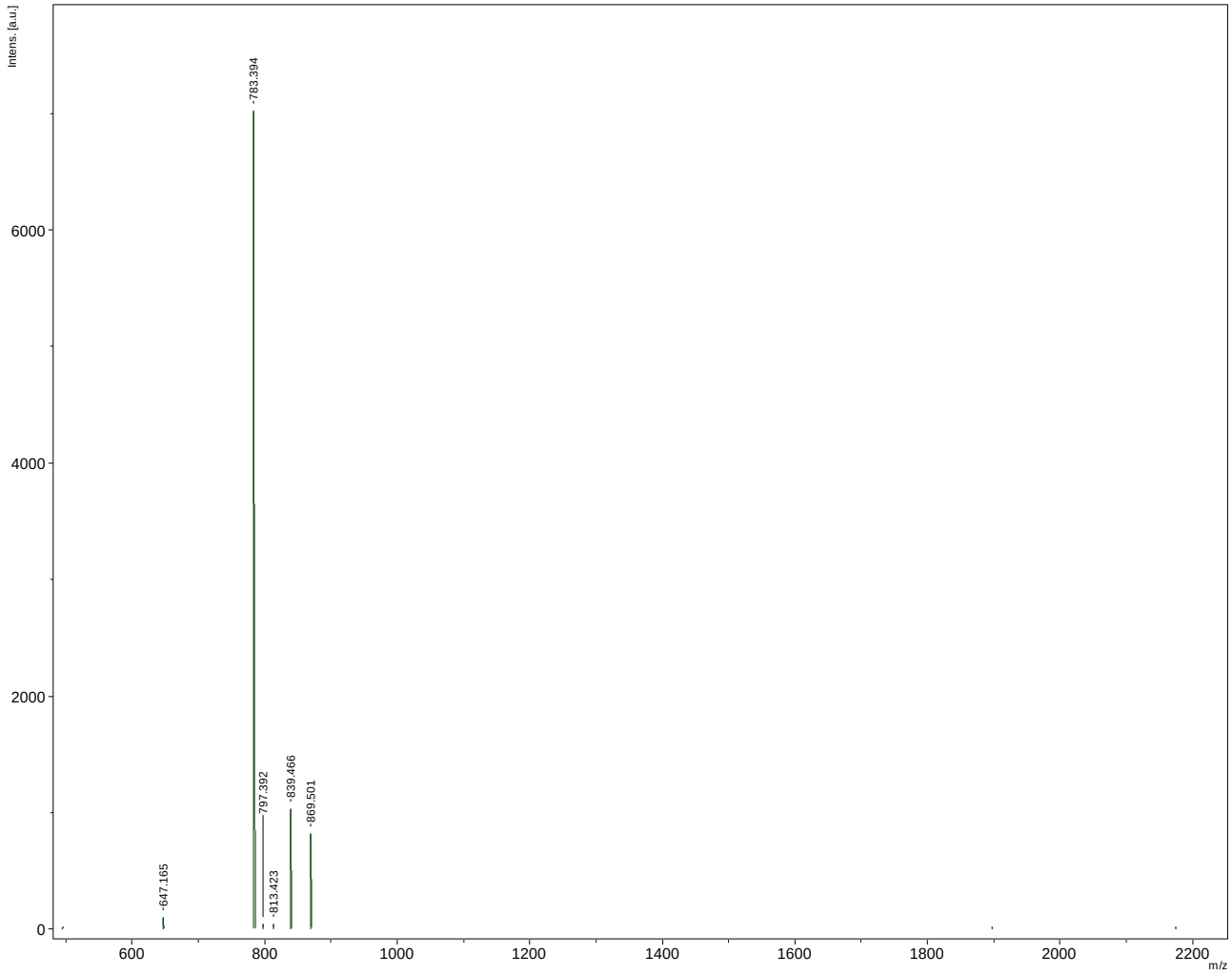

Figure S9. MALDI-TOF-MS spectrum in wide m/z range of **V990(tBP$^+$)(TFSI$^-$)**.

Oxidation of the V886

V886^{2+}(TFSI$^-$)$_2$

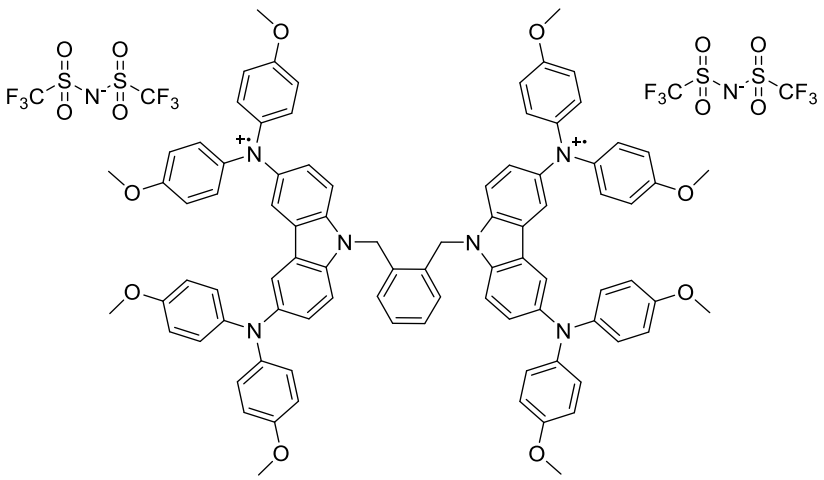

To a 500 mg (0.37 mmol) dissolved in 30 ml of DCM 288 mg (0.74 mmol) of AgTFSI was added. Solution immediately became deep blue-green. After stirring at room temperature for 24 h precipitated silver was filtered off through the plug of celite. DCM was evaporated, and resulting residue was precipitated from 20% solution in DCM into 15-fold excess of ether. The precipitate was filtered off and dried under vacuum resulting in the deep blue-green powder. Yield: 453 mg, 64.3%.

Anal. calcd for $C_{92}H_{76}F_{12}N_8O_{16}S_4$: C, 57.98; H, 4.02; N, 5.88; found: C, 57.78; H, 4.06; N, 5.94.

Pyridination of the $\mathbf{V886^{2+}(TFSI^-)_2}$

400 mg of $\mathbf{V886^{2+}(TFSI^-)_2}$ was dissolved in 1.5 ml of the freshly distilled tBP and the resulting solution was heated to 60^{o}C. After 20 min, when color changed from intensive blue-green to dark orange, tBP was distilled off on the rotorvapor. Residue was purified by column chromatography by using THF:*n*-hexane (1:4 v:v) as eluent, and consequentially strengthening it to the THF:*n*-hexane (3:2 v:v) eluent. Three products were separated (see full text for the description).

Yield of $\mathbf{V886(tBP^+)(TFSI^-)}$: 140 mg, 37.9%.

Yield of $\mathbf{V886(tBP^+)_2(TFSI^-)_2}$: 78 mg, 17.1%.

Yield of V886: 58 mg, 20.5%.

1-(9-{[2-({3,6-bis[bis(4-methoxyphenyl)amino]-9H-carbazol-9-yl}methyl)phenyl]methyl}-3,6-bis[bis(4-methoxyphenyl)amino]-9H-carbazol-4-yl)-4-tert-butylpyridin-1-ium bis(trifluoromethanesulfonyl)azanide; ***V886(tBP$^+$)(TFSI$^-$)***

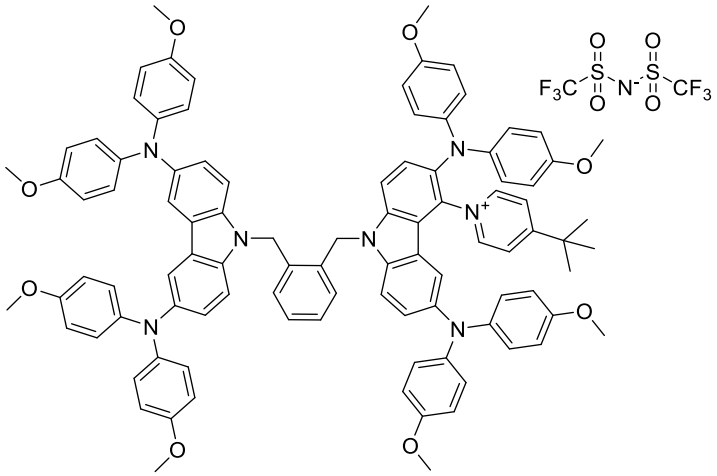

$\underline{R_f}$ =0.31; THF:*n*-hexane (3:2 v:v)

^{1}H NMR (400 MHz, DMSO-d_6) δ 9.04 (d, *J* = 6.5 Hz, 2H), 7.93 – 7.83 (m, 3H), 7.76 (d, *J* = 2.2 Hz, 2H), 7.56 – 7.46 (m, 3H), 7.39 (d, *J* = 8.8 Hz, 1H), 7.18 – 7.02 (m, 5H), 6.93 – 6.66 (m, 32H), 6.52 – 6.42 (m, 2H), 6.24 (d, *J* = 2.1 Hz, 1H), 5.99 (s, 2H), 5.92 (s, 2H), 3.72 – 3.66 (m, 24H), 1.22 (s, 9H).

^{13}C NMR (101 MHz, DMSO) δ 154.90, 154.68, 154.27, 142.02, 140.73, 140.53, 140.11, 137.49, 125.01, 124.58, 123.83, 123.49, 122.92, 121.08, 118.94, 117.88, 114.68, 55.27, 55.18, 55.05, 36.37, 29.20.

Anal. calcd for $C_{99}H_{88}F_6N_8O_{12}S_2$: C, 67.56; H, 5.04; N, 6.37; found: C, 67.42; H, 5.00; N, 6.39.

$C_{99}H_{89}F_6N_8O_{12}S_2$ [V886(tBP$^+$)(TFSI$^-$)+H$^+$] exact mass = 1759.5946 Da, observed mass MALDI-TOF-MS) = 1759.531 Da

$C_{97}H_{88}N_7O_8^+$ [V886(tBP$^+$)] exact mass = 1478.6694 Da, observed mass (MALDI-TOF-MS) = 1478.669 Da.

^{1}H NMR and ^{13}C NMR spectra of V886(tBP^{+})(TFSI^{-})

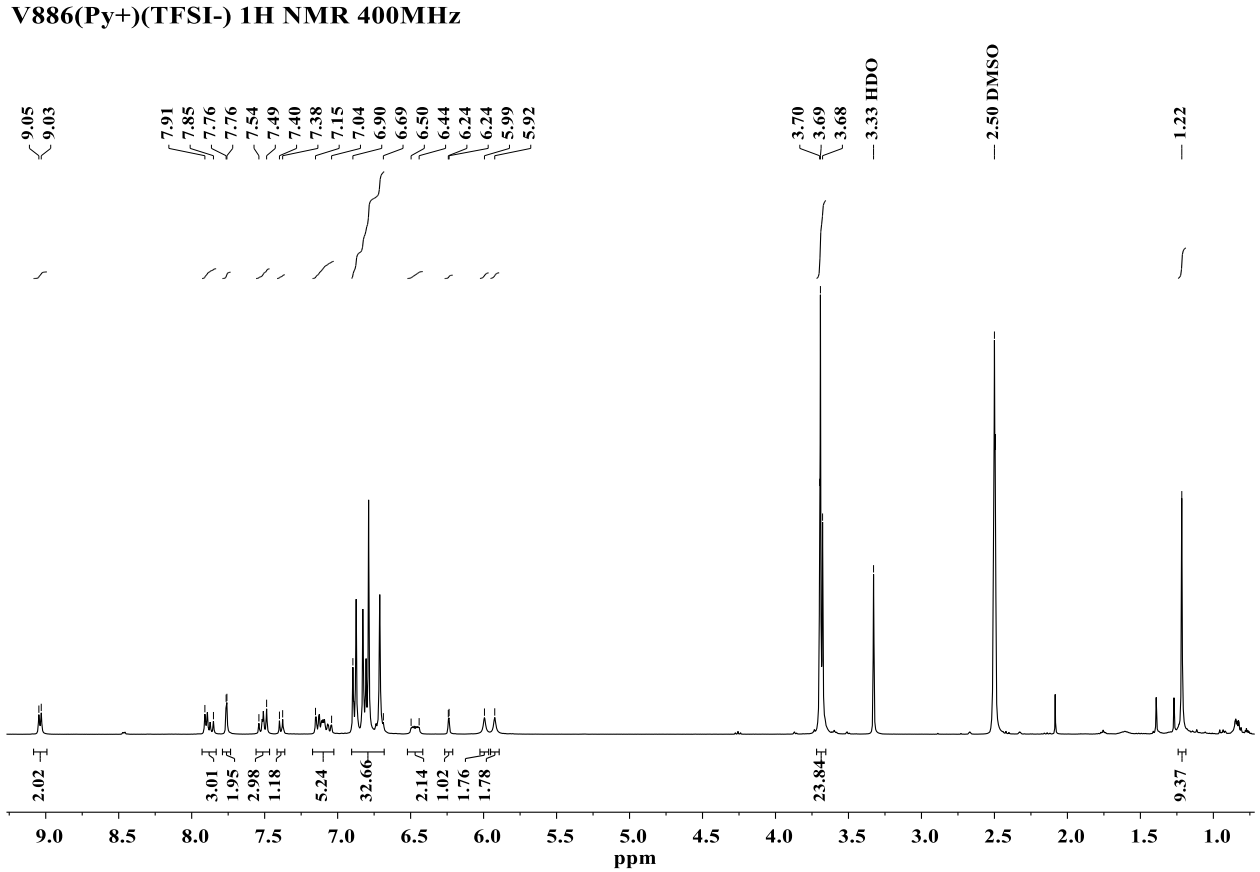

Figure S10. ^{1}H NMR spectrum of **V886(tBP^{+})(TFSI^{-})** from dmso-d6

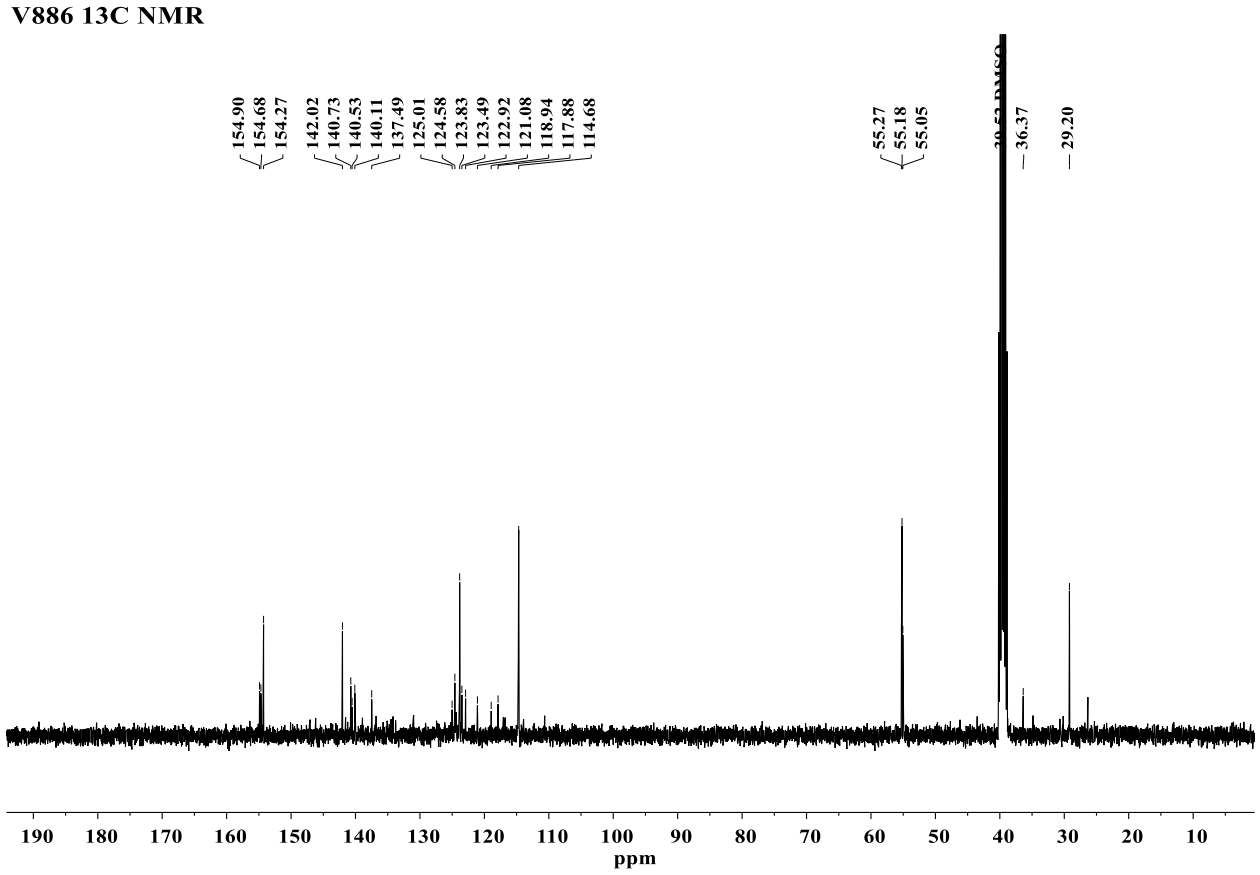

Figure S11. ^{13}C NMR spectrum of **V886(tBP^{+})(TFSI^{-})** from dmso-d6

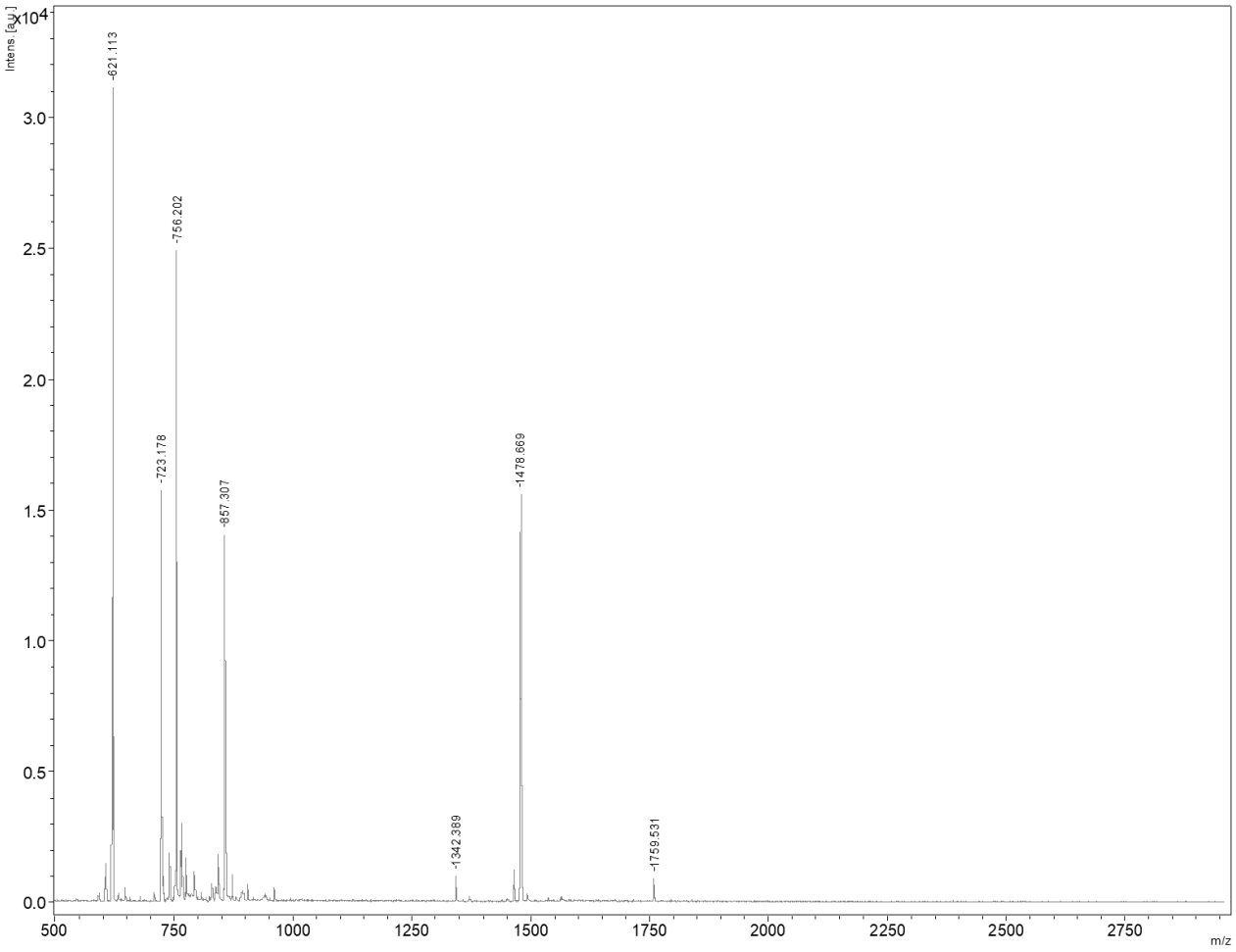

Figure S12. MALDI-TOF-MS spectrum in wide m/z range of **V886(tBP$^+$)(TFSI$^-$)**.

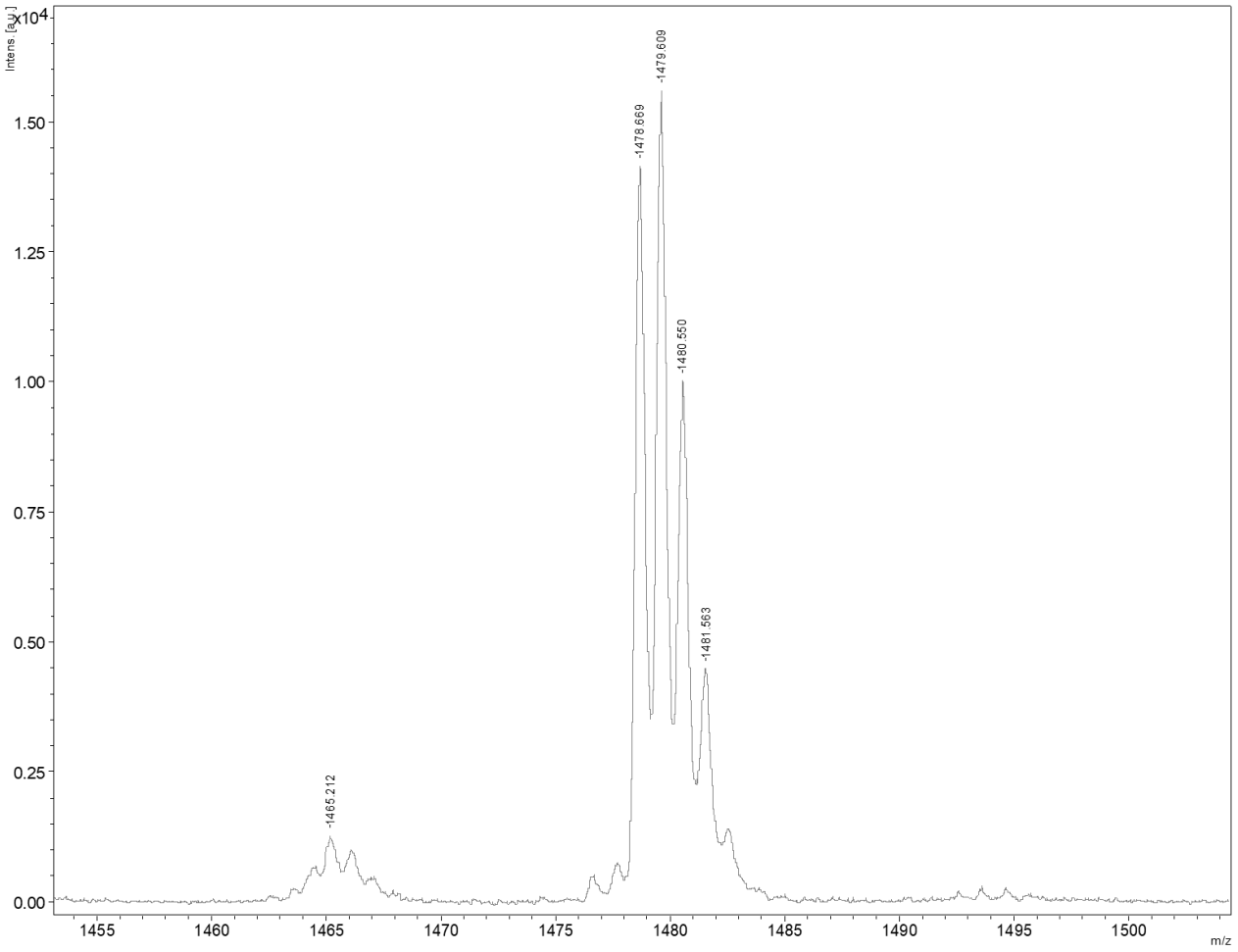

Figure S13. MALDI-TOF-MS spectrum in narrow m/z range of **V886(tBP$^+$)(TFSI$^-$)**.

1,1'-[1,2-phenylenebis(methylene{3,6-bis[bis(4-methoxyphenyl)amino]-9H-carbazole-9,4-diyl})]bis(4-tert-butylpyridin-1-ium) bis[bis(trifluoromethanesulfonyl)azanide]; ***V886(tBP$^+$)$_2$(TFSI$^-$)$_2$***

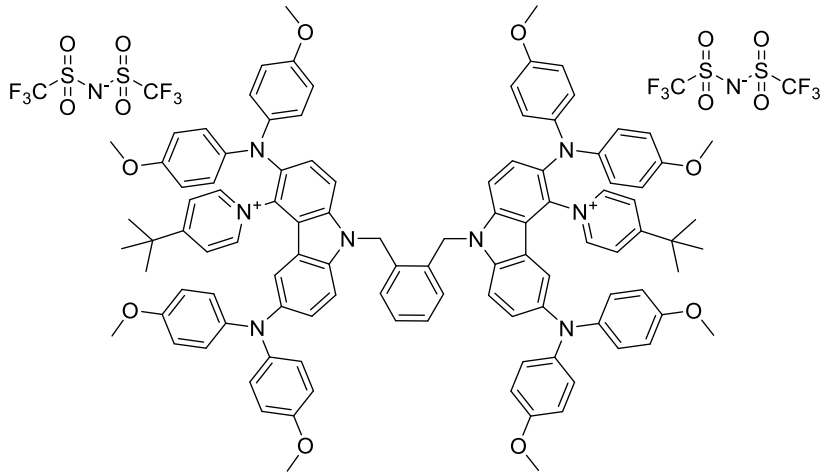

$\underline{R_f}$ =0.05; THF:*n*-hexane (3:2 v:v)

^{1}H NMR (400 MHz, DMSO-d_6) δ 9.05 (d, *J* = 6.4 Hz, 4H), 7.95 – 7.89 (m, 6H), 7.61 (d, *J* = 9.0 Hz, 2H), 7.42 (d, *J* = 8.8 Hz, 2H), 7.17 – 7.05 (m, 4H), 6.83 – 6.69 (m, 32H), 6.46 (dd, *J* = 5.6, 3.4 Hz, 2H), 6.25 (d, *J* = 2.1 Hz, 2H), 6.09 (s, 4H), 3.73 – 3.66 (m, 24H), 1.22 (s, 18H).

^{13}C NMR (101 MHz, DMSO) δ 154.90, 154.70, 146.17, 140.73, 140.11, 125.04, 124.59, 123.49, 114.73, 55.28, 55.07, 36.39, 29.20.

Anal. calcd for $C_{110}H_{100}F_{12}N_{10}O_{16}S_4$: C, 60.77; H, 4.64; N, 6.44; found: C, 60.56; H, 4.61; N, 6.48.

$C_{108}H_{100}F_6N_9O_{12}S_2^+$ [V886(tBP$^+$)$_2$(TFSI$^-$)] exact mass = 1892.6837 Da, observed mass (MALDI-TOF-MS) = 1892.588 Da.

^{1}H NMR and ^{13}C NMR spectra of V886(tBP^{+})$_2$(TFSI^{-})$_2$

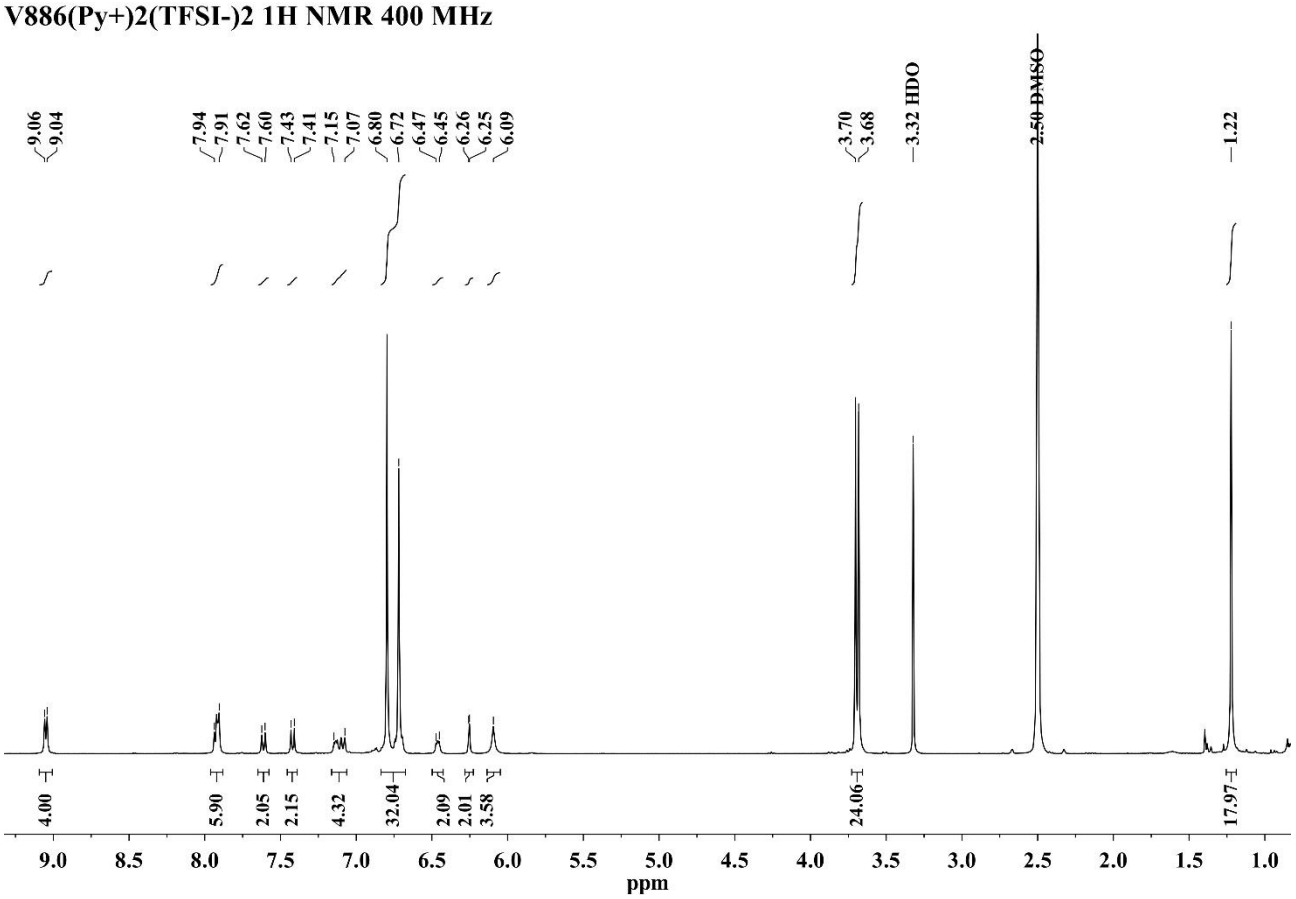

Figure S14. ^{1}H NMR spectrum of **V886(tBP^{+})$_2$(TFSI^{-})$_2$** from dmso-d6

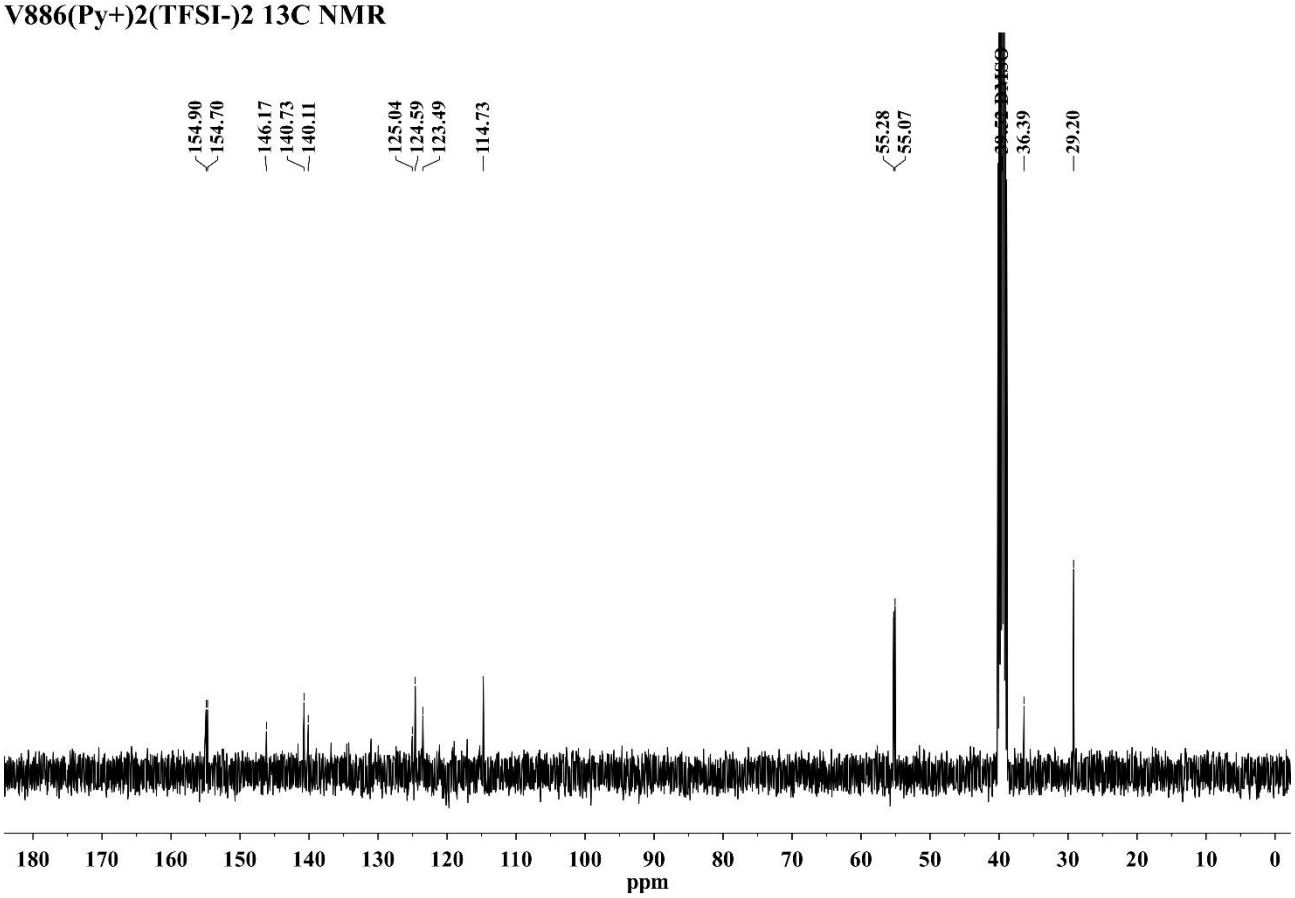

Figure S15. ^{13}C NMR spectrum of **V886(tBP^{+})$_2$(TFSI^{-})$_2$** from dmso-d6

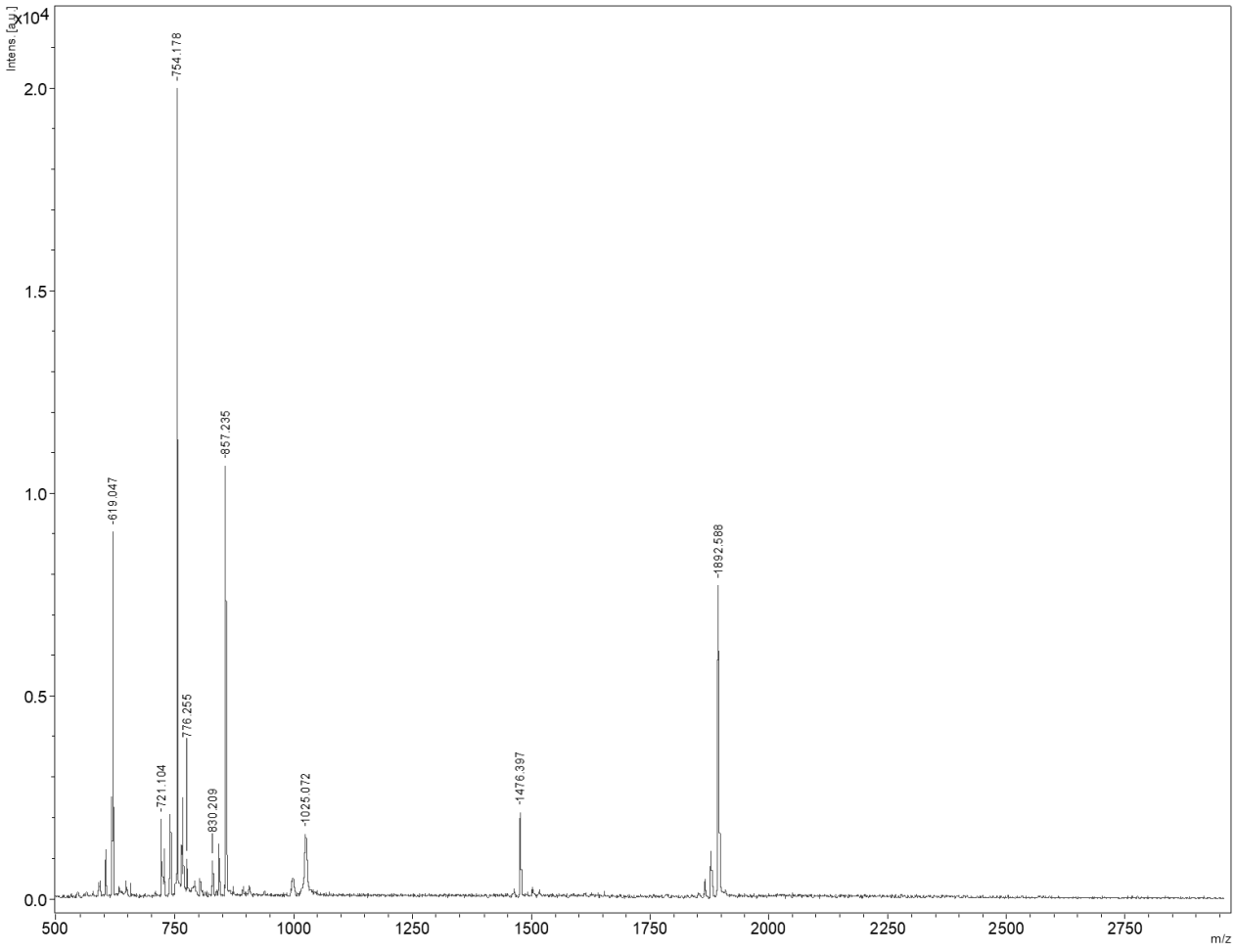

Figure S16. MALDI-TOF-MS spectrum in wide m/z range of **V886(tBP$^+$)$_2$(TFSI$^-$)$_2$**.

Ionization Potential Measurements

The solid state ionization potential (I_p) of the layers of the synthesized compounds was measured by the electron photoemission in air method[9–11]. The samples for the ionization potential measurement were prepared by dissolving materials in $CHCl_3$ and were coated on Al plates pre-coated with ~0.5 μm thick methylmethacrylate and methacrylic acid copolymer adhesive layer. The thickness of the transporting material layer was 0.5-1 μm. Usually photoemission experiments are carried out in vacuum and high vacuum is one of the main requirements for these measurements. If vacuum is not high enough the sample surface oxidation and gas adsorption are influencing the measurement results. In our case, however, the organic materials investigated are stable enough to oxygen and the measurements may be carried out in the air. The samples were illuminated with monochromatic light from the quartz monochromator with deuterium lamp. The power of the incident light beam was (2-5)×10^{-8} W. The negative voltage of –300 V was supplied to the sample substrate. The counter-electrode with the 4.5×15 mm^2 slit for illumination was placed at 8 mm distance from the sample surface. The counter-electrode was connected to the input of the BK2-16 type electrometer, working in the open input regime, for the photocurrent measurement. The 10^{-15} – 10^{-12} A strong photocurrent was flowing in the circuit under illumination. The photocurrent I is strongly dependent on the incident

light photon energy hν. The $I^{0.5}=f(h\nu)$ dependence was plotted. Usually the dependence of the photocurrent on incident light quanta energy is well described by linear relationship between $I^{0.5}$ and $h\nu$ near the threshold. The linear part of this dependence was extrapolated to the hν axis and I_p value was determined as the photon energy at the interception point.

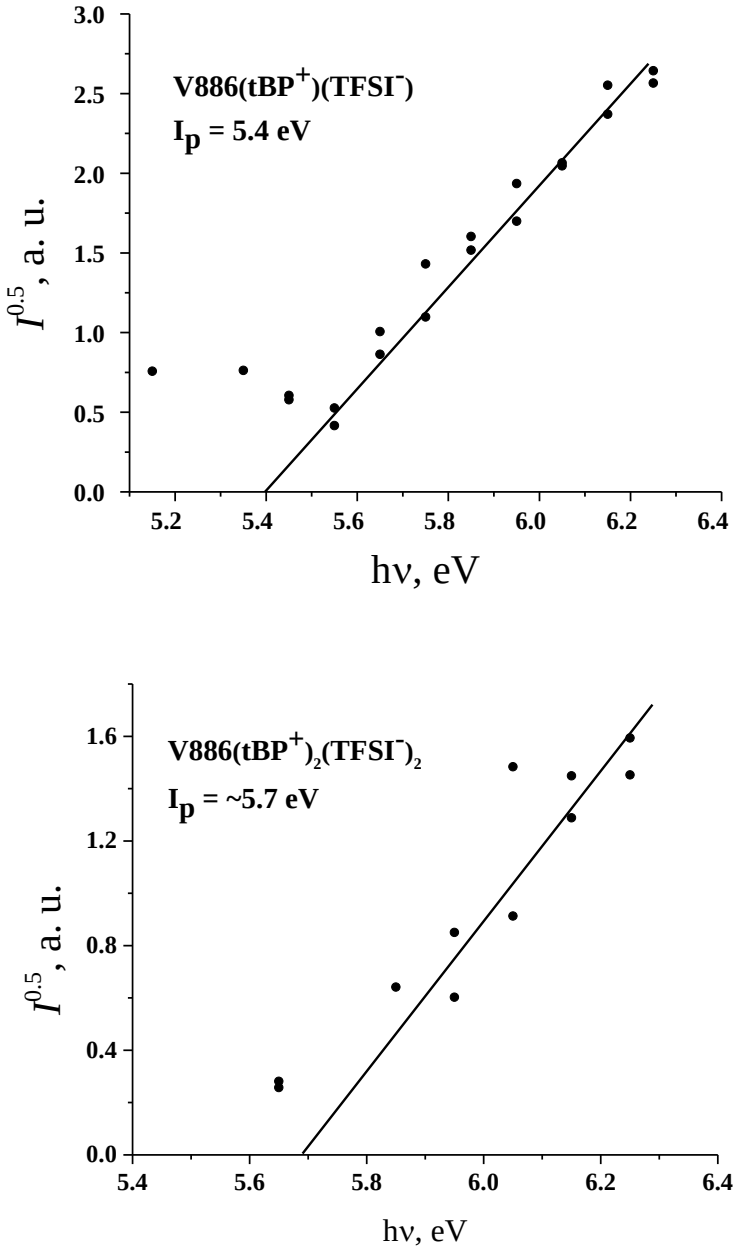

Figure S17. Photoemission in air spectra of the **V886(tBP$^+$)(TFSI$^-$)** (top), and **V886(tBP$^+$)$_2$(TFSI$^-$)$_2$** (bottom).

Cyclic voltammetry measurements

Electrochemical studies were carried out by a three-electrode assembly cell and potentiostat/galvanostat from Bio-Logic SAS. Measurements were carried out with a glassy carbon

electrode in acetonitrile solutions containing 0.1 M tetrabutylammonium hexafluorophosphate as electrolyte and Pt wire as the reference electrode, and a Pt wire counter electrode at a scan rate 50 mV×s^{-1}. Each measurement was calibrated with ferrocene (Fc).

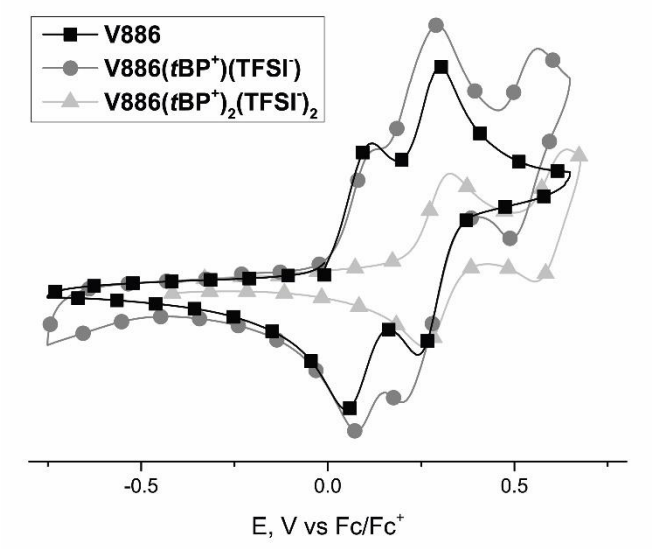

Figure S18. Cyclic voltammograms of V886-based compounds.

Table S1. Optical and electrochemical data of the V886, **V886(tBP$^+$)(TFSI$^-$)**, and **V886(tBP$^+$)$_2$(TFSI$^-$)$_2$**.

Material	E_{ox1}, V vs Fc	E_{ox2}, V vs Fc	E_{ox3}, V vs Fc	E_{HOMO} (eV)[a]	E_g^{opt} (eV)[b]	E_{LUMO} (eV)[c]	Ip (eV)	EA (eV)[d]
V886	0.0854	0.2717	-	-5.32	2.72	-2.60	5.04[12]	2.32
V886(tBP$^+$)(TFSI$^-$)	0.1077	0.2445	0.5270	-5.34	1.70	-3.64	5.4	3.7
V886(tBP$^+$)$_2$(TFSI$^-$)$_2$	0.2924	0.5989	-	-5.53	1.78	-3.75	5.7	3.92

[a]Conversion factors: ferrocene in THF vs SCE 0.56[13], SCE vs SHE: 0.244[14], SHE vs. vacuum: 4.43[15]. [b]Optical band gap (E_g^{opt}) was estimated from the edge of electronic absorption spectra from solution. [c]LUMO energy (E_{LUMO}) was calculated using equation $E_{LUMO} = E_{HOMO} + E_g^{opt}$. [d]Electron affinity (EA) calculated from the equation $EA = I_p - E_g^{opt}$.

Conductivity

For the estimation of materials bulk conductivity charge carriers extraction by linearly increasing voltage (CELIV) technique was used. Films were formed on pre-cleaned FTO substrate by drop-

casting 20 mg/ml solutions in acetonitrile. Aluminum electrodes were evaporated on top of the organic film and the measurements were conducted.

Table S2. Conductivities of the V886, **V886(tBP$^+$)(TFSI$^-$)**, and **V886(tBP$^+$)$_2$(TFSI$^-$)$_2$**.

Material	Conductivity, S×cm^{-1}
V886, doped with 10mol % FK209[7]	4.2×10^{-5}
V886(tBP$^+$)(TFSI$^-$)	1.0×10^{-9}
V886(tBP$^+$)$_2$(TFSI$^-$)$_2$	0.5×10^{-9}

UV/vis spectroscopy

UV/vis spectra were recorded on Shimadzu UV-3600 spectrometer from the 10^{-4} M solutions in THF.

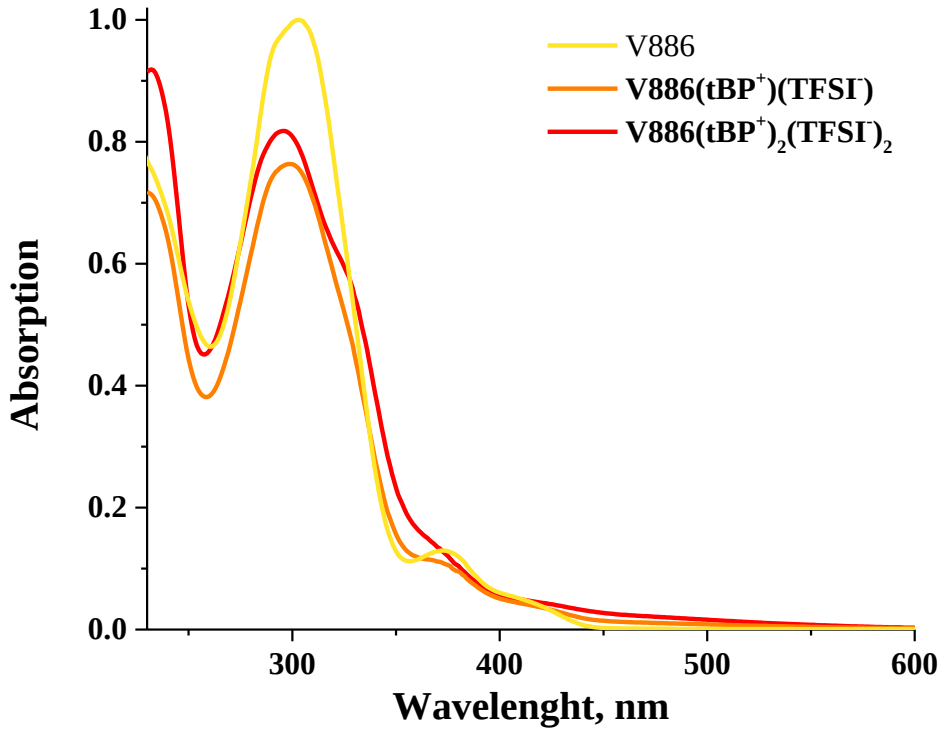

Figure S19. UV/vis spectra of the V886, **V886(tBP$^+$)(TFSI$^-$)**, and **V886(tBP$^+$)$_2$(TFSI$^-$)$_2$**.

Perovskite solar cell fabrication and characterization

Fluorine doped tin oxide (FTO) glass substrates (Nippon sheet glass) were sequentially cleaned with the detergent solution, acetone, and ethanol. Then, a compact TiO_2 layer was coated on the cleaned FTO substrate heated at 450 °C by spray pyrolysis deposition. A precursor solution was obtained by diluting titanium diisopropoxide (Sigma-Aldrich) in ethanol (0.6 mL; 10 mL). Mesoporous TiO_2 films were prepared using a diluted TiO_2 paste (Dyesol 30 NR-D) solution. Films were spin coated at 2000 rpm for 10 s and sintered on a hot plate at 500 °C for 30 min. After cooling to room temperature, films were treated with 0.1 M lithium bistrifluoromethanesulfonimidate solution (Li-TFSI, Aldrich) in acetonitrile by spin coating at 3000 rpm for 10 s and finally baked again at 500 °C for 30 min. The lead excess $(FAPbI_3)_{0.85}(MAPbBr_3)_{0.15}$ precursor solution was prepared by mixing FAI (1.1 M), PbI_2 (1.15 M), MABr (0.2 M), and $PbBr_2$ (0.2 M) in a mixed solvent of DMF:DMSO = 4:1 (volume ratio). Another solution of $CsPbI_3$ was also prepared as 1.15 M in DMF:DMSO (same volume ratio). For triple cations mixed perovskite solution, $(FAPbI_3)_{0.85}(MAPbBr_3)_{0.15}$ and $CsPbI_3$ solutions were mixed as 10 vol% ratio. The perovskite precursor solution was spin coated at 2000 rpm for 10 s, followed by 6000 rpm for 30 s. Trifluorotoluene (110 µL) was dropped on the spinning substrate at the 20 s in the second step. The films were annealed at 100 °C for 90 min in the glove box. The hole-transporting material was applied from a 40×10^{-3} M solution in chlorobenzene. Tert-butylpyridine (tBP), tris(2-(1H-pyrazol-1-yl)-4-tert-butylpyridine) cobalt(III) (FK209) and tris(bis(trifluoromethylsulfonyl)imide) (Li-TFSI) were added as additives. Equimolar amounts of additives were added: 330 mol% tBP, 50 mol% Li-TFSI from a 1.8 M stock solution in acetonitrile and 3 mol% FK209 from a 0.25 M stock solution in acetonitrile. Finally, 70 nm of Au was deposited by thermal evaporation as the back electrode.

The solar cell measurement was done using commercial solar simulators (Oriel VeraSol-2, AAA class LED). The light intensity was calibrated with a Si reference cell equipped with an IR-cutoff filter (KG3, Newport) and it was recorded before each measurement. Current–voltage characteristics of the cells were obtained by applying an external voltage bias while measuring the current response with a digital source meter (Keithley 2400/2604). The voltage scan rate was 20 mV s^{-1} and no device preconditioning such as light soaking or forward voltage bias was applied before starting the measurement. The cells were masked with the active area of 0.16 cm^2 to fix the active area and reduce the influence of the scattered light.

More detailed description of the perovskite solar cells characteristics can be found in our recent publication.[12]

Perovskite solar cell aging

PSC aging was performed by keeping device under thermal stress (at 80°C in the oven) for 340h.

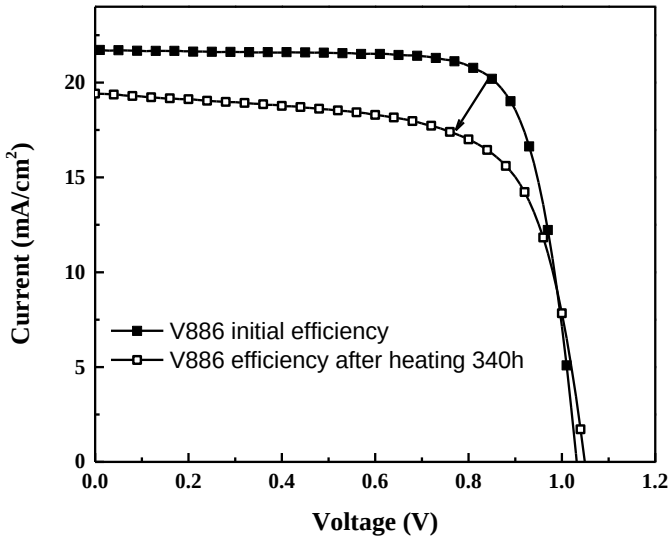

Figure S20. J-V characteristics of PSC with **V886** as a HTM before and after aging at 80^{o}C for 340 h.

MS analysis of the aged device

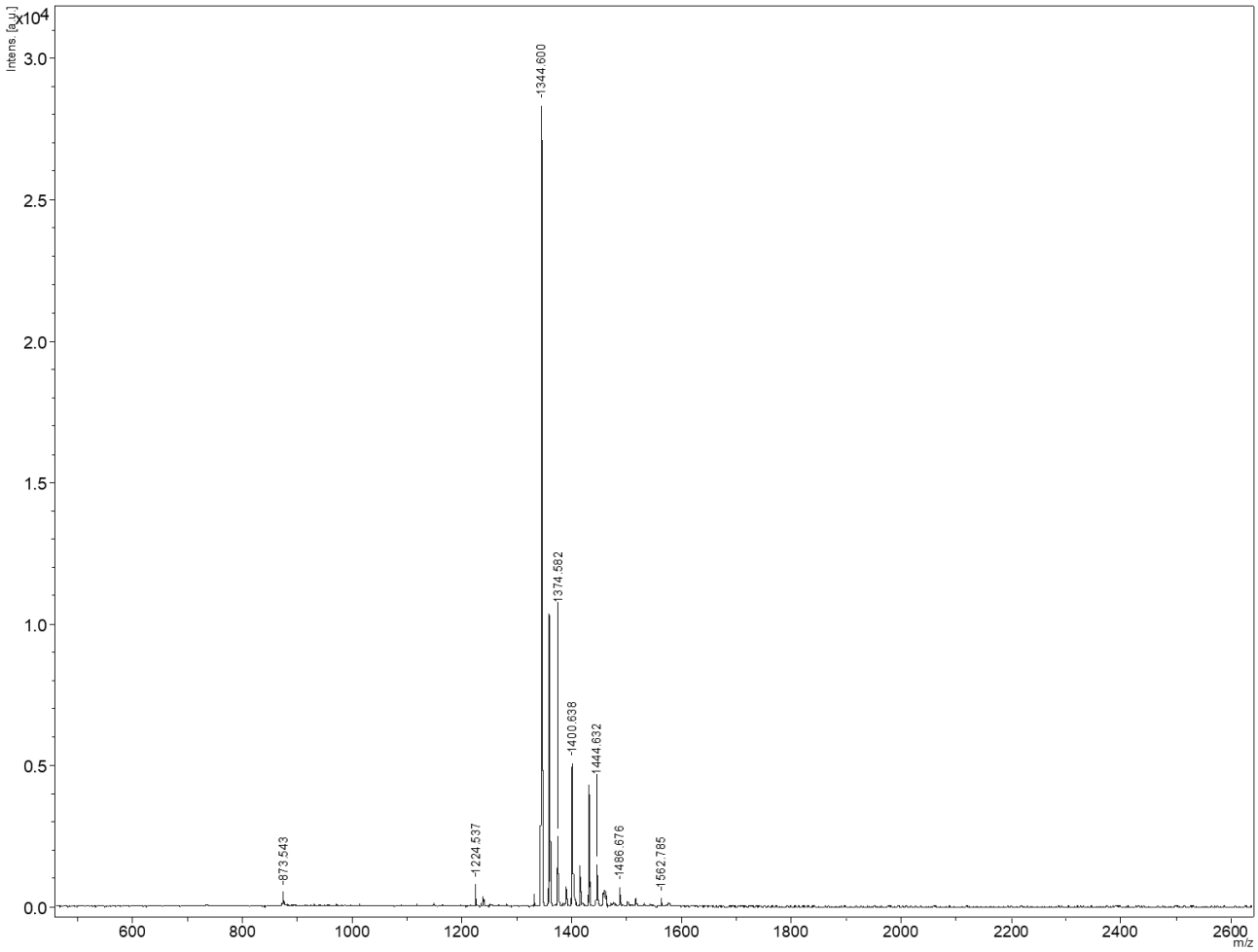

Figure S21. MALDI-TOF-MS spectrum in wide m/z range of HTM layer, washed from the V886-based PSC, aged at 80 ºC for 340 h.

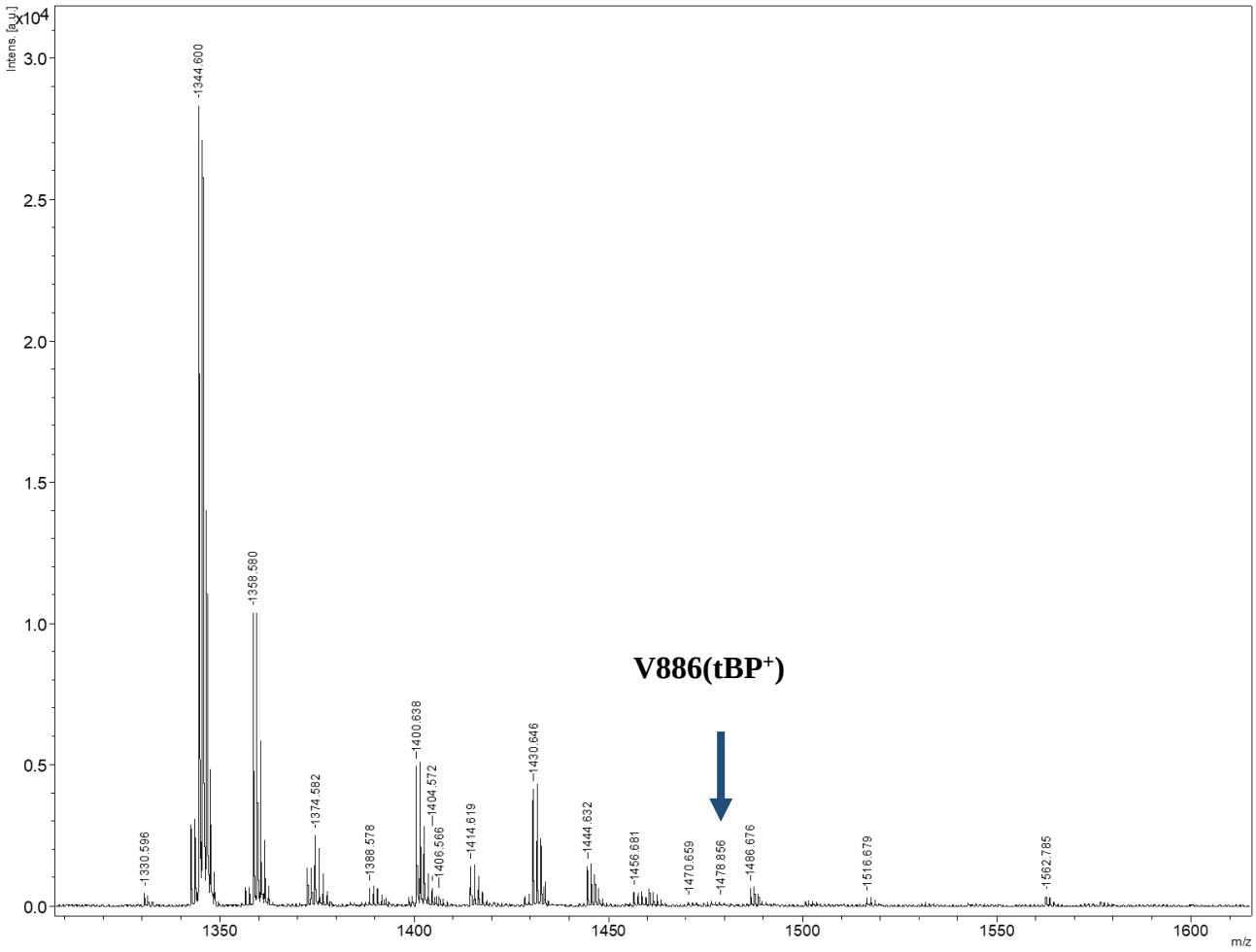

Figure S22. MALDI-TOF-MS spectrum in narrow m/z range of HTM layer, washed from the V886-based PSC, aged at 80 ºC for 340 h.

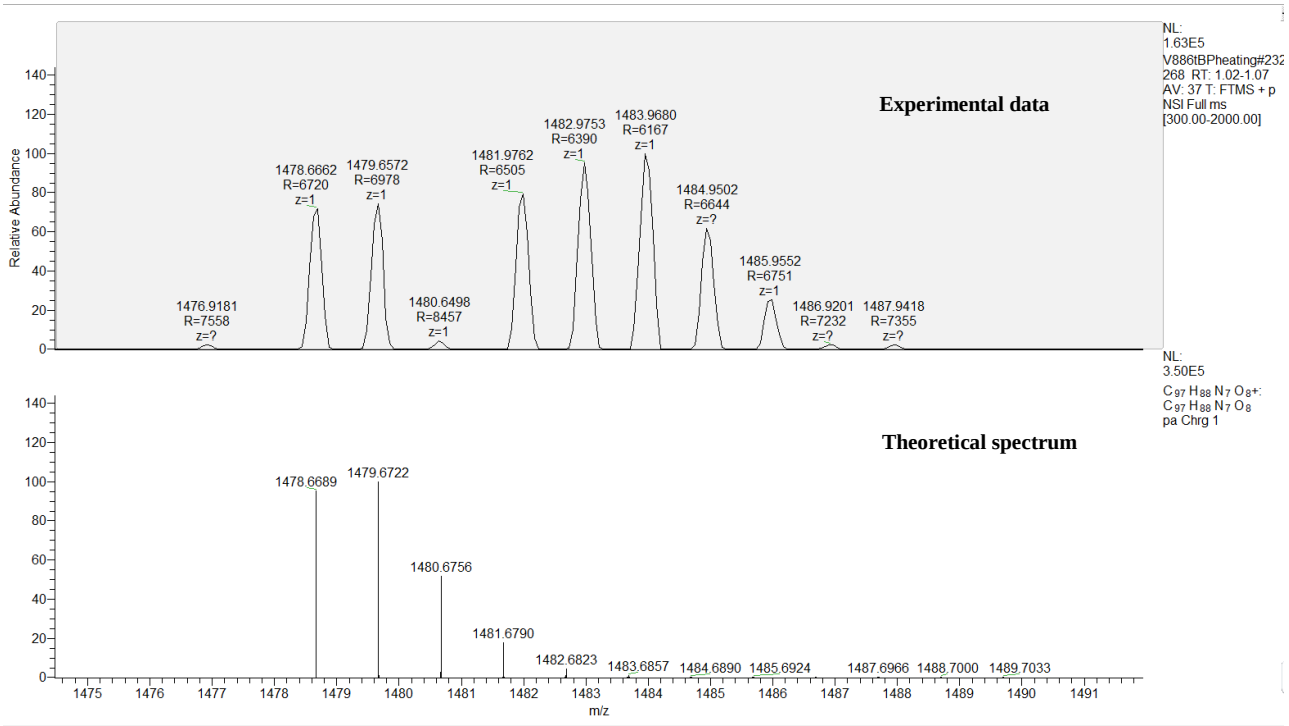

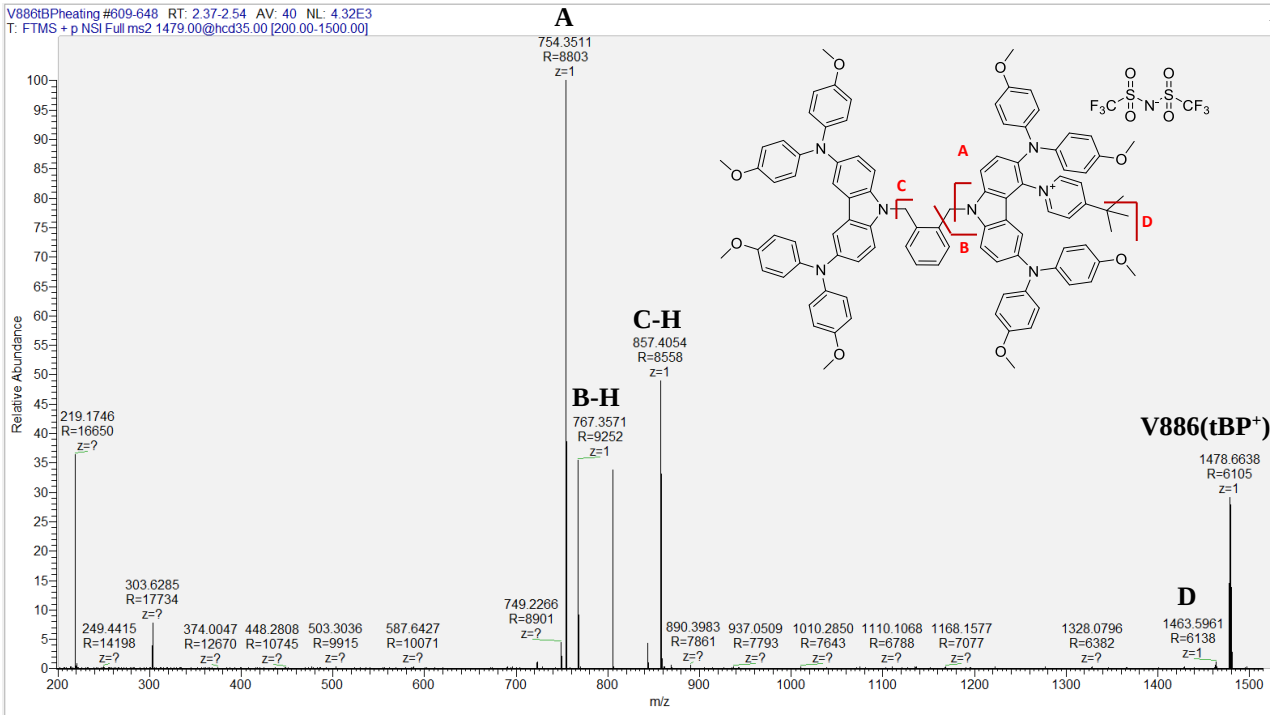

Figure S23. Full MS and MS/MS spectra of 1478.856 m/z signal (**V886(tBP$^+$)** in narrow and wide m/z ranges, respectively. MS/MS spectrum includes tentative fragmentation map and assigned fragments.

References

1 R. Ahlrichs, M. Bär, M. Häser, H. Horn and C. Kölmel, *Chem. Phys. Lett.*, 1989, **162**, 165–169.

2 C. Lee, W. Yang and R. G. Parr, *Phys. Rev. B*, 1988, **37**, 785–789.

3 A. D. Becke, *J. Chem. Phys.*, 1993, **98**, 5648–5652.

4 A. Schäfer, H. Horn and R. Ahlrichs, *J. Chem. Phys.*, 1992, **97**, 2571–2577.

5 F. Weigend, R. Ahlrichs, K. A. Peterson, T. H. Dunning, R. M. Pitzer and A. Bergner, *Phys. Chem. Chem. Phys.*, 2005, **7**, 3297.

6 C. Steffen, K. Thomas, U. Huniar, A. Hellweg, O. Rubner and A. Schroer, *J. Comput. Chem.*, 2010, **31**, 2967–2970.

7 P. Gratia, A. Magomedov, T. Malinauskas, M. Daskeviciene, A. Abate, S. Ahmad, M. Grätzel, V. Getautis and M. K. Nazeeruddin, *Angew. Chemie Int. Ed.*, 2015, **54**, 11409–11413.

8 P.-M. Huang, J.-S. Li, X.-M. Duan, T. Zeng, X.-L. Yan and IUCr, *Acta Crystallogr. Sect. E Struct. Reports Online*, 2005, **61**, o2366–o2367.

9 M. Cordona and L. Ley, *Top. Appl. Phys.*, 1978, **26**, 1.

10 E. Miyamoto, Y. Yamaguchi and M. Yokoyama, *Electrophotography*, 1989, **28**, 364.

11 M. Kirkus, M.-H. Tsai, J. V. Grazulevicius, C.-C. Wu, L.-C. Chi and K.-T. Wong, *Synth. Met.*, 2009, **159**, 729–734.

12 P. Gratia, A. Magomedov, T. Malinauskas, M. Daskeviciene, A. Abate, S. Ahmad, M. Grätzel, V. Getautis and M. K. Nazeeruddin, *Angew. Chemie - Int. Ed.*, 2015, **54**.

13 N. G. Connelly and W. E. Geiger, *Chem. Rev.*, 1996, **96**, 877–910.

14 V. V Pavlishchuk and A. W. Addison, *Inorganica Chim. Acta*, 2000, **298**, 97–102.

15 H. Reiss and A. Heller, *J. Phys. Chem.*, 1985, **89**, 4207–4213.